Mémoire d'Habilitation à Diriger des Recherches

Spécialité : *Astrophysique*

présenté par

Jonathan Ferreira

OOOOOOOOOOOOOOOOOOOOOOOOOOOOOOOOOOOOOOOO

Description Dynamique et Quelques Diagnostics Observationnels des Structures Magnétiques d'Accrétion-Ejection

OOOOOOOOOOOOOOOOOOOOOOOOOOOOOOOOOOOOOOOO

Soutenue le 4 Juillet 2007 devant la commission composée de

Mr. Gilles Henri	Président
Mr. Max Camenzind	Rapporteur
Mr. Michel Tagger	Rapporteur
Mr. Kanaris Tsinganos	Rapporteur
Mr. Henri-Claude Nataf	Examinateur
Mr. Christophe Sauty	Examinateur

Laboratoire d'AstrOphysique de Grenoble, BP53X F-38041 Grenoble
Université Joseph Fourier

Table des matières

Chapitre 1

Introduction

1.1 The accretion-ejection phenomenon

Accretion-ejection is an important aspect of two major questions in modern astrophysics, namely (i) star and planets formation and (ii) high energy production in the vicinity of black holes. Our knowledge in these two topics will greatly improve thanks to new instruments such as AMBER/VLTI, ALMA on one side and INTEGRAL, AUGER, GLAST on the other. But accretion-ejection is also tackling fundamental questions in physics : magnetic turbulence and chaos, plasma confinement and related instabilities, dynamo effect (magnetic field generation), particle acceleration etc...

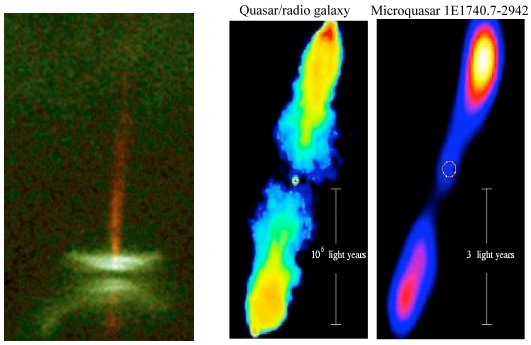

FIG. 1.1 – Jets in astrophysics.

Figure 1.1 shows typical jets from different astrophysical sources. Bipolar jets from young stars (left), mostly seen in optical lines (in red), are supersonic and come from the innermost regions close to the star, hidden here by the opaque circumstellar disc seen edge on. The disc material is in quasi-keplerian

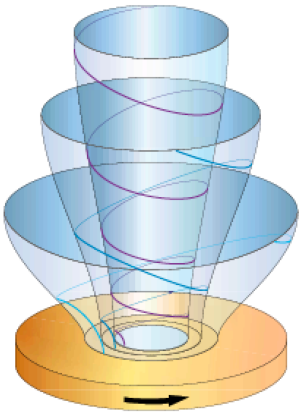

FIG. 1.2 – Picture of a Magnetized Accretion-Ejection Structure. The disc rotation gives rise to a shear of the magnetic field lines (in blue) which provokes a magnetic torque. Energy and angular momentum are therefore transferred to the field, allowing thereby accretion to proceed. This energy is given back to the fraction of the disc material which has been lifted out and gives rise to fast bipolar jets, confined by their own magnetic field.

rotation and spirals slowly towards the young forming star increasing thereby its mass (contrary to the Earth which stays at the same orbit around the Sun). This inward motion is called accretion. It manifests itself through a typical radiation signature emitted by the infalling disc material. A tight correlation between accretion and ejection signatures shows that these two processes are interdependent.

Accretion-ejection also occurs around a compact object, namely a black hole or a neutron star. The other two images in figure 1.1 show bipolar jets observed in radio wavelengths. The middle one is a jet from a radio galaxy or a quasar, emitted from an accretion disc settled around a supermassive black hole, several million to billion times the mass of the Sun. The rightmost image shows bipolar jets coming from the disc around a galactic stellar black hole, looking very similar to quasar jets. Because many characteristics seem to scale with the central black hole mass, such an object has been nicknamed a "microquasar".

1.2 Personal contribution

Although it was soon recognized (in the 80's) that ejection and accretion were tightly related, a truly self-consistent model appeared only lately. It was

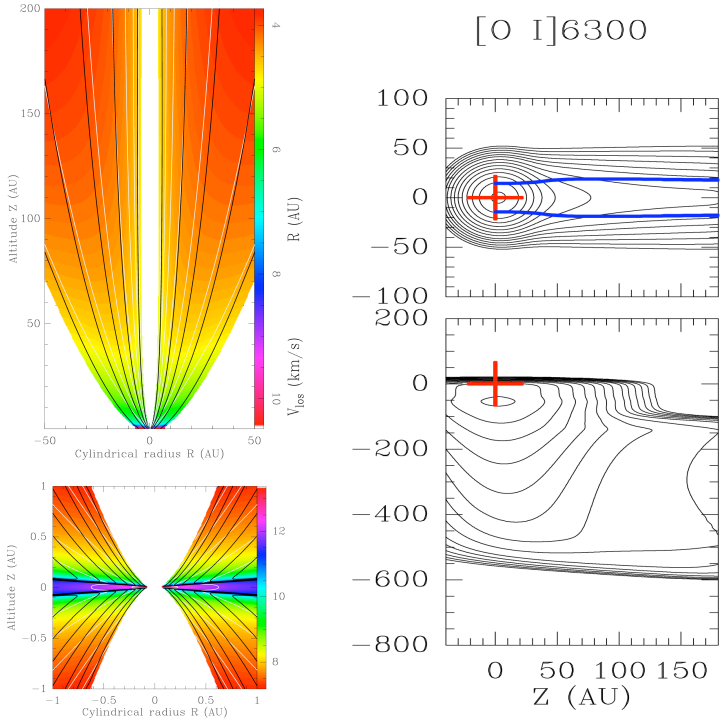

FIG. 1.3 – **Left :** Self-similar model of a MAES around a one solar mass star. Colors are density contours (in cm^{-3}), streamlines are shown in black, total velocity isocontours in white (Ferreira 1997). **Right :** Synthetic image and position-velocity diagram from the same model in the [O I]6300 line, as it would be observed with the Hubble Space Telescope. The cross shows the star position (Garcia et al 2001b).

my PhD work (Ferreira & Pelletier 93a,b, 95), continued during my post-doc (Ferreira 97) and completed with Fabien Casse, my own PhD student (Casse & Ferreira 2000a,b, Ferreira & Casse 2004). This is the only published magneto-hydrodynamic (MHD) model that describes in a self-consistent way the physics of an accretion disc thread by a large scale magnetic field, giving rise to self-collimated jets (figure 1.2). Such a system was called a Magnetized Accretion-Ejection Structure, hereafter MAES. This model is unique in the sense that it provides both the physical conditions required to steadily launch jets and the distributions of all quantities in space (although the self-similar assumption used introduces unavoidable biases).

Several fruitful collaborations were then undergone with observers and modelers of jets from young stars (Cabrit et al 1999, Garcia et al. 2001a,b,

Pesenti et al. 2003, 2004) . Indeed, observations of these objects put already very severe constraints on the models (figure 1.3). In this community, there was still a debate on the driving engine of jets : was it the disc alone (MAES), the star alone (stellar winds) or some star-disc interaction ? Thanks to our work and new observations motivated by it, a consensus has slowly emerged. It is now accepted that most of the ejected mass in jets comes from the accretion disc (MAES), even if other ejection events are certainly coexisting (see Ferreira et al 2006b for more details).

I would like to stress that the physics of MAES has been confirmed by two independent groups, using two distinct numerical MHD codes (figure 1.4). My self-similar MAES solutions are now being used by two PhD thesis (Linda Podio at Firenze with A. Natta and Despina Panoglou at Porto with P. Garcia and S. Cabrit). In collaboration with F. Masset, it has been shown that the density drop at the radial transition between an outer standard accretion disc and a MAES will stop the inward migration of proto-planetary cores (Masset et al. 2006). This is of crucial importance for planet formation. Actually, the study of the impact of a MAES in the innermost disc regions (say from 0.1 to several astronomical units) around a protostar is only starting.

The whole MAES picture requires of course the presence of a large scale magnetic field in the disc. This is very difficult to measure, in any astrophysical object. Donati et al. (2005) did this *tour de force* using the spectropolarimeter ESPadOnS (my input on this nice work was only in the interpretation). There is now a clear evidence that the protostar FU Ori has indeed such a large scale magnetic field anchored in the disc. Extending this detection to a broader range of objects is clearly of primordial importance.

Chapter 2 is devoted to the theory of magnetized accretion discs driving jets with a focus on young stellar objects. I first introduce observational and theoretical arguments in favor of the "disc wind" paradigm. There, accretion and ejection are interdependent, requiring therefore to revisit the standard picture of accretion discs. A simple magnetostatic approach is shown to already provide some insights of the basic phenomena. The magnetohydrodynamic equations as well as all usual assumptions are then clearly listed. The relevant physical mechanisms of steady-state accretion and ejection from Keplerian discs are explained in a model independent way. The results of self-similar calculations are shown and critically discussed, for both cold and warm jet configurations. I finally provide observational predictions and the physical conditions required in circumstellar discs. This part is a slightly modified version of a lecture given at a CNRS winter school in Aussois, France (Ferreira 2002). Although some time has passed by since the school (it was held in 2000), all conclusions remain valid and it accurately describes the core of my work. However, references are clearly a bit outdated. I introduced in

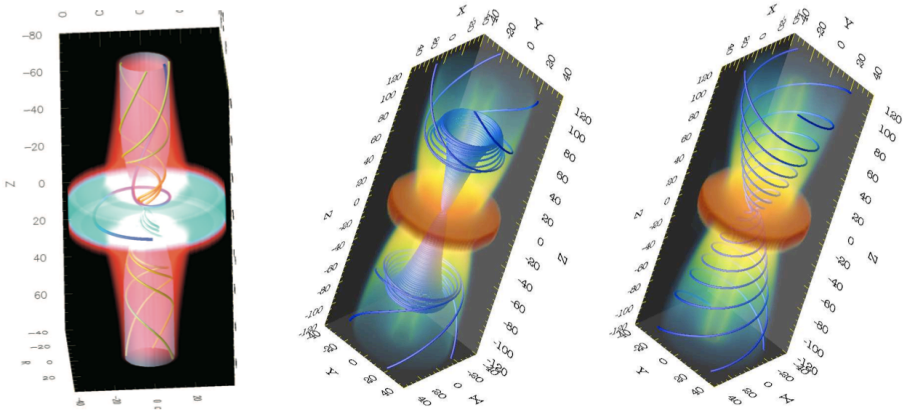

FIG. 1.4 – **Left :**First MHD simulation of a MAES, done with the MHD code VAC (Casse & Keppens 2002, 2004). The numerical experiment has confirmed that only an equipartition field can drive steady jets. **Right :** Two simulations done with the AMR MHD code FLASH (Zanni et al. 2004). Another important analytical result is confirmed : only a large magnetic diffusivity allows a steady state (rightmost image).

the text some more recent references but interested readers are respectfully invited to consult Ferreira et al. (2006a) for black hole X-ray binaries and Ferreira et al. (2006b) for young stars.

Chapter 3 describes very briefly my two main projects, namely the study of (a) the star-disc magnetic interaction and (b) the spectral and temporal properties of black hole X-ray binaries. In some sense, they are both an extension of my previous work. The former addresses the connection with the central star while the second focuses on time-dependent accretion-ejection events. In fact, both projects nourish each other : the work on young stars can then be naturally applied to magnetized neutron stars or white dwarves whereas time-dependent accretion-ejection will be obviously very interesting for young stars, especially for FU Orionis like objects.

Chapitre 2

Magnetized accretion discs driving jets

2.1 Some preliminary questions

Collimated ejection of matter is widely observed in several astrophysical objects : inside our own galaxy from all young forming stars and some X-ray binaries, but also from the core of active galaxies. All these objects share the following properties : jets are almost cylindrical in shape ; the presence of jets is correlated with an underlying accretion disc surrounding the central mass ; the total jet power is a sizeable fraction of the accretion power.

2.1.1 Why should jets be magnetized ?

There are basically two kinds of jet observations : spectra (continuum and blue shifted emission lines) and images (in the same lines for Young Stellar Objects -hereafter YSO-, or in radio continuum for compact objects). Most of these images show jets that are extremely well collimated, with an opening angle of only some degrees. On the other hand, the derived physical conditions show that jets are highly supersonic. Indeed, emission lines in YSO jets require a temperature of order $T \sim 10^4$ K, hence a sound speed $C_s \sim 10$ km/s while the typical jet velocity is $v_j \sim 300$ km/s. The opening angle θ of a ballistic hydrodynamic flow being simply $\tan\theta = C_s/v_j$, this provides $\theta \sim 5^o$ for YSOs, nicely compatible with observations. Thus, jets could well be ballistic, showing up an inertial confinement. But the fundamental question remains : **how does a physical system produce an unidirectional supersonic flow ?** Naively, this implies that confinement must be closely related to the acceleration process.

This has soon been recognized in the Active Galactic Nuclei or AGN community (where jets were being observed for quite a long time, see Bridle & Perley 1984), leading Blandford & Rees to propose in 1974 the "twin-exaust" model. In this model, the central source is emitting a spherically symmetric jet, which is confined and redirected into two bipolar jets by the external pressure gradient. Indeed, the rotation of the galaxy would probably produce a disc-like anisotropic distribution of matter around its center. Thus, in principle, the ejected plasma could be focused towards the axis of rotation of the galaxy (where there is less matter there) and thereby accelerated like in a De Laval nozzle. Such an idea was afterwards applied by Cantó (1980) and Königl (1982) for YSOs. However, this model had severe theoretical drawbacks, related to Kelvin-Helmholtz instabilities quickly destroying the nozzle. Besides, it does not explain the very origin of the spherical flow.

But the strongest argument comes from more recent observations, like those of HH30 (see eg. Ray et al. 1996). We know now that jets are already clearly collimated close to the central star (eg at roughly 30 AU), with no evidence of any relevant outer pressure. This implies that jets must be self-collimated. In my opinion, such an observation also rules out the proposition that jets are collimated by an outer poloidal magnetic field (Spruit et al. 1997).

The only model capable of accelerating plasma along with a self-confinement relies on the action of a large scale magnetic field carried along by the jet. In fact, Lovelace and Blandford proposed independently in 1976 that if a large scale magnetic field would thread an accretion disc, then it could extract energy and accelerate particules (electron positron pairs in their models). Then, Chan & Henriksen (1980) showed, using a simplified configuration, that such a field could indeed maintain a plasma flow collimated. But it was Blandford & Payne who, in 1982, produced the first full calculation of the interplay between a plasma flow (made of electrons and protons) and the magnetic field, showing both acceleration and self-collimation.

2.1.2 What is the jet driving source ?

To make a long story short, there are three different situations potentially capable of driving magnetized jets from young forming stars[1].

– **the protostar alone** : these purely stellar winds extract their energy from the protostar itself (eg. Mestel 1968, Hartmann & McGregor 1980,

[1]An alternative model is based on some circulation of matter during the early infall stages (see Lery et al. 1999 and references therein). However, by construction, such a model is only valid for Class 0 sources and cannot be used to explain jets from T-Tauri stars. See also Contopoulos & Sauty (2001).

Sauty et al. 2002,2004).

- **the accretion disc alone** : "disc winds" are produced from a large radial extension in the disc, thanks to the presence of a large scale magnetic field (eg. Blandford & Payne 1982, Pudritz & Norman 1983). They are fed with both matter and energy provided by the accretion process alone.
- **the interaction zone between the disc and the protostar** : these "X-winds" are produced in a tiny region around the magnetopause between the disc and the protostar (eg. Shu et al. 1994,1995, Shang et al 1998, 2002, Lovelace et al. 1999, Ferreira et al. 2000).

Purely stellar wind models are less favoured because observed jets carry far too much momentum. In order to reproduce a YSO jet, a protostar should be either much more luminous or rotating faster than observations show (DeCampli 1981, Königl 1986). This leaves us with either disc-winds or X-winds[2]. From the observational point of view, it is very difficult to discriminate between these two models. In a review, Livio (1997) gathered a number of arguments for the disc wind model. The main idea is to look for a model able to explain jets from quite a lot of different astrophysical contexts (YSOs, AGN, X-ray binaries). The only "universal" ingredient required is an accretion disc threaded by a large scale magnetic field. Such a paradigm naturally explains (qualitatively) all accretion-ejection correlations known and is consistent with every context : young stars (Cabrit et al 1990, Hartigan et al 1995), microquasars (eg. Mirabel & Rodriguez 1999, Fender et al. 2004) and AGN (see eg. Serjeant et al. 1998, Cao & Jiang 1999, Jones et al. 2000).

2.1.3 Where does this magnetic field come from ?

Let's face it : we don't know. There are two extreme possibilities. The first one considers that the field has been advected by the infalling material, leading to a flux concentration in the inner disc regions. The second one relies on a local dynamo action in the disc. Most probably, the answer lies between these two extreme cases.

If the interstellar magnetic field has been indeed advected, the crucial issue is the amount of field diffusion during the infall. Indeed, if we take the fiducial values $n \sim 1$ cm^{-3} and $B \sim 4\ \mu$G of dense clouds and use the law $B \propto n^{1/2}$ (Crutcher 1999), we get a magnetic field at 1 UA ranging from 10 to 10^3

[2]Camenzind and collaborators proposed an "enhanced" version of stellar winds, related to an old idea of Uchida & Shibata (1984). In this picture, a magnetospheric interaction with the accretion disc is supposed to strongly modify both jet energetics and magnetic configuration, leading to enhanced ejection from the protostar (Camenzind 1990, Fendt et al. 1995, Breitmoser & Camenzind 2000, Matt & Pudritz 2005b and references therein).

G ! One must then consider in a self-consistent way the dynamical influence of the magnetic field, along with matter energy equation and ionization state. This is something extremely difficult and, as far as I know, no definite result has been yet obtained (see however Banerjee & Pudritz 2006).

How exactly disc dynamo works is also quite unclear. Dynamo theory remains intricate, relying on the properties of the turbulence triggered inside the disc. In our current picture of accretion discs, these are highly turbulent because of some instability, probably of magnetic origin (see Balbus 2003). Such a turbulence is believed to provide means of efficient transport inside the disc, namely anomalous viscosity, magnetic diffusivity and heat conductibility. Obviously, small scale (not larger than the disc vertical scale height), time dependent magnetic fields will then exist inside accretion discs. But we are interested in the mean flow (hence mean field) dynamics. So, in practice what does ejection require ? To produce two opposedly directed jets, there must be a large scale magnetic field in the disc, which is open and of one of the following topologies :

Dipolar : the field threads the disc, with only a vertical component at the disc midplane, matter being forced to cross the field lines while accreting (eg. Blandford & Payne 1982).

Quadrupolar : field lines are nearly parallel to matter, entering the disc in its plane and leaving it at its surfaces, with only a non zero azimuthal component at the disc midplane (eg. Lovelace et al. 1987).

Most jet models and numerical simulations assume a dipolar magnetic configuration, with no justification. In fact, it turns out from the analysis of disc physics that only the dipolar configuration is suitable for launching jets from keplerian accretion discs (see appendix A in Ferreira 1997). This has been recently confirmed using α dynamo-generated magnetic fields (Rekowski et al. 2000). This is due to a change of sign of the α effect across the disc midplane, as observed in numerical simulations of MHD turbulence in the shearing box approximation (Brandenburg & Donner 1997). But a realistic situation requires to treat both turbulence and the backreaction of the magnetic field in a self-consistent way. Indeed, jet production is a means of flux leakage, hence of possible dynamo self-regulation (Yoshizawa & Yokoi 1993). Anyway, this severe issue of dynamo and turbulence lead theorists to simply assume the existence of a large scale magnetic field. Its' value and distribution are then either imposed or obtained as conditions for stationarity in Magnetized Accretion-Ejection Structures (MAES).

2.1.4 The Magnetized Accretion-Ejection Structure paradigm

A large scale (mean) magnetic field of bipolar topology is assumed to thread an accretion disc, allowing ejected plasma to flow along open field lines. This field extracts both angular momentum and energy from the underlying disc and transfers them back to the ejected plasma. There have been numerous studies of magnetized jets (e.g. Blandford & Payne 1982, Heyvaerts & Norman 1989, Pelletier & Pudritz 1992, Contopoulos & Lovelace 1994, Rosso & Pelletier 1994, Lery et al. 1999 to cite only a few), but they all suppose that the underlying disc would support the jets. In all these works, the disc itself was treated as a boundary condition, generally assuming a standard viscous accretion disc (Shakura & Sunyaev 1973). However, if jets are to carry away the disc angular momentum, they strongly influence the disc dynamics.

The investigation of MAES, where accretion and ejection are interdependent, requires a new theory of accretion discs. The relevant questions that must be addressed by any realistic model of stationary magnetized accretion-ejection structures are the following :

(1) What are the relevant physical mechanisms inside the disc ?

(2) What are the physical conditions allowing accretion and ejection ?

(3) Can we relate jet properties to those of the disc ?

To answer these questions, one must take into account the full 2D problem (not 3D, thanks to axisymmetry) and **not** treat the disc as infinitely thin as in a standard disc theory. As a consequence, no toy-model has been able yet to catch the main features of these accretion-ejection structures. There, the disc accretion rate exhibits a radial variation as matter is being ejected. The link between accretion and ejection in a MAES can therefore be measured by the quantity

$$\xi = \frac{d \ln \dot{M}_a}{d \ln r} \tag{2.1}$$

called the "ejection index". This parameter (which can vary within the disc) measures the local ejection efficiency. In a standard accretion disc, $\xi = 0$ everywhere leading to a constant accretion rate. A complete theory of MAES must provide the allowed values of ξ as a function of the disc properties.

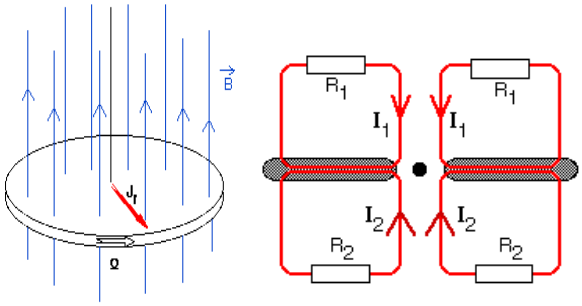

FIG. 2.1 – **Left** : A rotating disc embedded in a magnetic field induces a current leading to a magnetic braking (Barlow's wheel). **Right** : A MAES can be seen as two independent electric circuits, each corresponding to a jet. Asymmetric jets can thus be easily achieved, even with a symmetric poloidal field (with R_1 and R_2 different, arising from a different jet-ambiant medium interaction) .

2.2 Theoretical framework of MAES

2.2.1 A magnetostatic approach

The Barlow experiment

A wheel made of a conducting material is put between the two poles of an electromagnet. This device produces a magnetic field perpendicular to the disc, along its axis of rotation. The wheel brushes against mercury contained in a tank, thereby allowing to close an electric circuit (mercury, wire connecting the disc axis, the disc itself). In order to check if some current is flowing, we can put a small lamp. With a crank, we then provide a rotating motion to the disc and let it evolve. If the magnetic field is off, nothing happens : the lamp stays mute (no current) and the disc very gradually slows down. On the contrary, if the magnetic field is present, the lamp lights on (a current is flowing) and the disc stops very quickly ! When the disc is finally motionless, the lamp is also off.

The explanation of this phenomenon lies in electromagnetic induction. The disc is made of a conducting material, meaning that charged particules are free to move inside it. When the disc starts to rotate, these particules drag the magnetic field along with them. The field lines become then twisted, showing a conversion of mechanical into magnetic energy. Once the disc has stopped, all the initial mechanical energy has been converted (dissipated into heat along the whole electric circuit). The magnetic field was just a mediator

between different energy reservoirs.

On the importance of currents

A MAES is an astrophysical Barlow wheel. Indeed, the rotation of a conducting material in a static magnetic field B_z induces an electric (more precisely electromotive) field

$$\vec{E}_m = \vec{u} \wedge \vec{B} \simeq \Omega r B_z \vec{e_r} \tag{2.2}$$

where Ω is the matter angular velocity and $\vec{e_r}$ the radial unit vector (in cylindrical coordinates). This field produces an electromotive force e, ie a difference of voltage between the inner r_i and outer r_e disc radii, namely

$$e = \int_{r_i}^{r_e} \vec{E}_m \cdot \vec{dr} \simeq \Omega_i r_i^2 B_i \tag{2.3}$$

(where the dominant contribution is assumed to arise at the inner radius). In steady state, two electric circuits can develop (above and below the disc midplane) with a current $I_\pm = e/Z_\pm$ where $Z_\pm$ is their impedance. There is therefore an available electric power

$$P = e(I_- + I_+) = \frac{\Omega_i^2 r_i^4 B_i^2}{Z_{eq}} \tag{2.4}$$

where Z_{eq} is the equivalent impedance. Since a current $I = I_- + I_+$ is flowing inside the disc, it becomes affected by the magnetic field through the Laplace force $\vec{F} = \int_{r_i}^{r_e} I \vec{dr} \wedge \vec{B}$, which provides a torque acting against the disc rotation. This result is consistent with Lenz's law, which states that induced currents work against the cause that gave birth to them.

Now, the existence of such a torque allows matter to fall towards the central engine, hence to be accreted. Energy conservation implies that the mechanical power liberated through accretion, namely

$$P_{acc} = \frac{GM\dot{M}_a}{2r_i} \ , \tag{2.5}$$

where $\dot{M}_a$ is the accretion rate, must be equal to the electric power P. This imposes an impedance matching

$$Z_{eq} = \frac{2r_i^2 B_i^2}{\dot{M}_a} \sim \mu_o \sqrt{\frac{GM}{r_i}} \tag{2.6}$$

where μ_o is the vacuum permeability. The rhs estimate used a magnetic field close to equipartition with the thermal energy inside the disc (see Sect 5.2.2). The disc accretion rate depends therefore on the global electric circuit.

Electric currents $I_\pm$ flow along the axis, more precisely are distributed inside the jets. But if we model such current as being carried by an electric wire, we can estimate the generated magnetic field, namely $B_\phi(r) = -\mu_o I/2\pi r$. Such a field is negative, consistent with the shear given by the disc rotation. Because of this field, there is a Laplace force towards the axis, ie the famous "hoop stress" which maintains the jets collimated.

To summarize :

1. **Accretion** : a torque due to the magnetic field extracts the disc angular momentum. Such a torque is related to the establishment of two parallel electric circuits. Their equivalent impedance is directly linked to the accretion rate affordable by the structure.
2. **Global energy budget** : a fraction of the accretion power is dissipated into Joule heating (disc and jets heating, allowing radiation), another is converted into kinetic power carried by the jets.
3. **Jet acceleration** : possible due to the conversion of electric into kinetic power. Note that if the impedances Z_+ and Z_- (which describe all dissipative effects) are different, then two bipolar but *asymmetric* jets can be produced.
4. **Jet collimation** : jets do have naturally a self-collimating force *if they carry a non-vanishing current*. Since the electric circuit must be closed, not all magnetic field lines embrace a non-zero current. This obviously implies that all field lines anchored in the disc cannot be self-collimated (Okamoto 1999, 2003).

Lots of physics can be understood within the framework of magnetostatics. However, the precise description of a rotating astrophysical disc, its interrelations with outflowing plasma as well as the calculation of the asymptotic current distribution inside the jets (necessary to understand collimation) quite evidently require a fluid description.

2.2.2 Magnetohydrodynamics

Magnetohydrodynamics (MHD) describes the evolution of a collisional ionized gas (a plasma) submitted to the action of an electromagnetic field. Because the source of the field lies in the motions of charged particules (currents), the field is intrinsically tied to and dependent of these motions. Therefore, because of this high non-linearity, MHD offers an incredible amount of behaviours.

From a multicomponent to a single fluid description

Circumstellar discs and their associated jets are made of dust and gas, which is composed of different chemical species of neutral elements, ions and electrons. We should therefore make a multicomponent treatment. However, this is far too complex especially when energetics comes in. On the other hand, if all components are well coupled (through collisions) a single fluid treatment becomes appropriate.

For each specie α, we define its numerical density n_α, mass m_α, electric charge q_α, velocity $\vec{v}_\alpha$ and pressure P_α. The equation of motion for each species writes

$$\rho_\alpha \frac{d\vec{v}_\alpha}{dt} = -\vec{\nabla} P_\alpha - \rho_\alpha \vec{\nabla}\Phi_G + \sum_\beta \vec{F}_{\beta\alpha} + n_\alpha q_\alpha (\vec{E} + \vec{v}_\alpha \wedge \vec{B}) \tag{2.7}$$

where $d./dt = \partial./\partial t + \vec{v}_\alpha \cdot \nabla$ is the Lagrangean derivative, $\rho_\alpha = n_\alpha m_\alpha$, Φ_G is the gravitational potential of the central star and $\vec{F}_{\beta\alpha}$ is the collisional force due to all other species β. We can define the "mean" flow very naturally as

$$\begin{aligned} \rho &= \sum_\alpha n_\alpha m_\alpha \\ \rho\vec{u} &= \sum_\alpha m_\alpha n_\alpha \vec{v}_\alpha \\ P &= \sum_\alpha n_\alpha k_B T \\ \vec{J} &= \sum_\alpha n_\alpha q_\alpha \vec{v}_\alpha \end{aligned} \tag{2.8}$$

where ρ is the density, $\vec{u}$ the velocity, P the pressure, $\vec{J}$ the current density and k_B the Boltzmann constant. A single fluid description becomes relevant whenever the plasma is enough collisional. In such a case, we can safely assume that all species share the same temperature T. Moreover, we assume that any drift between the mean flow and a specie α is negligible, namely $\|\vec{v}_\alpha - \vec{u}\| \ll \|\vec{u}\|$. Using Newton's second law ($\sum_{\alpha,\beta} \vec{F}_{\alpha\beta} = \vec{0}$) and local electrical neutrality ($\sum_\alpha n_\alpha q_\alpha = 0$), we get the usual dynamical equations for one fluid

$$\frac{\partial \rho}{\partial t} + \nabla \cdot \rho\vec{u} = 0 \tag{2.9}$$

$$\rho \frac{d\vec{u}}{dt} = -\nabla P - \rho \nabla \Phi_G + \vec{J} \wedge \vec{B} \tag{2.10}$$

by summing over all species α. Even if the bulk of the flow is made of neutrals, they feel the magnetic force through collisions with ions (mainly) and

electrons, $\vec{J} \wedge \vec{B} = (1+X)(\vec{F}_{in} + \vec{F}_{en})$ where $X = \rho_i/\rho_n$ is the density ratio of ions to neutrals.

The evolution of the electromagnetic field is described by Maxwell's equations, namely (in vacuum)

$$\nabla \cdot \vec{B} = 0 \tag{2.11}$$

$$\nabla \wedge \vec{B} = \mu_o \vec{J} + \frac{1}{c^2}\frac{\partial \vec{E}}{\partial t} \tag{2.12}$$

$$\nabla \cdot \vec{E} = \frac{\rho_*}{\varepsilon_o} \tag{2.13}$$

$$\nabla \wedge \vec{E} = -\frac{\partial \vec{B}}{\partial t} \tag{2.14}$$

where $\rho_* = \sum_\alpha n_\alpha q_\alpha$ is the electric charge density. Faraday's law (Eq. 2.14) shows that the strength of the electric field varies like $E/B \sim L/t \sim U$ where U is a typical plasma velocity. Now, using Ampère's equation (2.12), shows that the displacement current has an effect of order $(U/c)^2$ only with respect to real currents (c is the speed of light). Thus, in a non-relativistic plasma, it can be neglected providing a current density

$$\vec{J} = \frac{1}{\mu_o}\nabla \wedge \vec{B} \tag{2.15}$$

directly related to the magnetic field. Under this approximation, electric charge conservation

$$\frac{\partial \rho_*}{\partial t} + \nabla \cdot \vec{J} = 0 \tag{2.16}$$

shows that no charge accumulation is allowed : the first term is also of order $(U/c)^2$. Therefore $\nabla \cdot \vec{J} = 0$, implying closed electric circuits.

Energy conservation of the electromagnetic field writes

$$\frac{\partial W}{\partial t} + \nabla \cdot \vec{S}_{MHD} = -\vec{J} \cdot \vec{E} \tag{2.17}$$

where $W = W_e + W_m = \varepsilon_o E^2/2 + B^2/2\mu_o$ is the electromagnetic field energy density and

$$\vec{S}_{MHD} = \frac{\vec{E} \wedge \vec{B}}{\mu_o} \tag{2.18}$$

is the Poynting vector, carrying the field energy remaining after interaction with the plasma (the term $\vec{J} \cdot \vec{E}$). Inside the non-relativistic framework, the energy density contained in the electric field is negligible with respect to W_m (of order $(U/c)^2$).

Generalized Ohm's law

In order to close the above system of equations, we need to know the electric field $\vec{E}$. Its expression is obtained from the electrons momentum equation, consistently with the single fluid approximation. Namely, we assume that electrons are so light that they react almost instantaneously to any force, i.e.

$$\vec{0} = -\nabla P_e \ + \ \sum_\beta \vec{F}_{\beta e} - e n_e (\vec{E} + \vec{v}_e \wedge \vec{B}) \tag{2.19}$$

$$\vec{E} + \vec{u} \wedge \vec{B} \ = \ (\vec{u} - \vec{v}_e) \wedge \vec{B} - \frac{\nabla P_e}{e n_e} + \sum_\beta \frac{m_\beta n_\beta \nu_{\beta e}}{e n_e} (\vec{v}_\beta - \vec{v}_e) \tag{2.20}$$

where $\nu_{\beta e}$ is the collision frequency of a specie β on electrons. Now, using (i) the expression of the Lorentz force $\vec{J} \wedge \vec{B}$, (ii) the approximation $\vec{J} \simeq e n_e (\vec{v}_i - \vec{v}_e)$ and (iii) neglecting the contribution due to the collisions between electrons and neutrals (with respect to those involving ions), we obtain the generalized Ohm's law

$$\vec{E} \ + \ \vec{u} \wedge \vec{B} = \eta \vec{J} \ + \ \frac{\vec{J} \wedge \vec{B}}{e n_e} \ - \ \left(\frac{\rho_n}{\rho} \right)^2 \frac{(\vec{J} \wedge \vec{B}) \wedge \vec{B}}{m_{in} n_i \nu_{in}} \ - \ \frac{\nabla P_e}{e n_e} \tag{2.21}$$

where $\eta = (m_{ne} n_n \nu_{ne} + m_{ie} n_i \nu_{ie})/(e n_e)^2$ is the electrical (normal) resistivity due to collisions, and $m_{\alpha\beta}$ the reduced mass. The first term on the rhs is the Ohm term, the second is the Hall effect, the third the ambipolar diffusion term and the fourth a source of electric field due to any gradient of electronic pressure. Fortunately, all these terms become negligible with respect to $\vec{u} \wedge \vec{B}$ whenever the plasma is well coupled and ionized ($\rho_n \ll \rho$).

Plasma energy equation

This is the trickiest equation and it can be written in several forms. We choose to express the internal energy equation, which can be written as

$$\rho T \frac{dS}{dt} = \Gamma - \Lambda \tag{2.22}$$

where S is the plasma specific entropy, Γ all heating terms and Λ all cooling terms. Note that a transport term (eg. such as heat conduction) can cool down the plasma somewhere and heat it up elsewhere. The MHD heating rate due to the interaction between the plasma and the electromagnetic field writes

$$\Gamma_{MHD} = \vec{J} \cdot (\vec{E} + \vec{u} \wedge \vec{B}) \simeq \eta J^2 + \left(\frac{\rho_n}{\rho} \right)^2 \frac{\left| \vec{J} \wedge \vec{B} \right|^2}{m_{in} n_i \nu_{in}} \tag{2.23}$$

The first term is the Joule effect while the second is the heating due to ambipolar diffusion. Although dynamically negligible in discs, such an effect might be responsible for jets heating (Safier 1993, Garcia et al. 2001a,b).

2.2.3 Modelling a MAES

Assumptions

Our goal is to describe an accretion disc threaded by a large scale magnetic field of bipolar topology. In order to tackle this problem, we will make several symplifing assumptions :

(i) Single-fluid MHD : matter is ionized enough and all species are well coupled. As a consequence, we use the simple form of Ohm's law

$$\vec{E} + \vec{u} \wedge \vec{B} = \eta \vec{J} \tag{2.24}$$

Taking the curl of this equation and using Faraday's law, we get the induction equation providing the time evolution of the magnetic field

$$\frac{\partial \vec{B}}{\partial t} = \nabla \wedge (\vec{u} \wedge \vec{B}) - \nabla \wedge (\nu \nabla \wedge \vec{B}) \tag{2.25}$$

where $\nu = \eta/\mu_o$ is the magnetic diffusivity. The first term describes the effect of advection of the field by the flow while the second describes the effect of diffusion, matter being able to cross field lines thanks to diffusivity.

(ii) Axisymmetry : using cylindrical coordinates (r, ϕ, z) no quantity depends on ϕ, the jet axis being the vertical axis. As a consequence $E_\phi = 0$ and all quantities can be decomposed into poloidal (the (r, z) plane) and toroidal components, eg. $\vec{u} = \vec{u_p} + \Omega r \vec{e_\phi}$ and $\vec{B} = \vec{B_p} + B_\phi \vec{e_\phi}$. A bipolar magnetic configuration can then be described with

$$\vec{B_p} = \frac{1}{r} \nabla a \wedge \vec{e_\phi} \ , \tag{2.26}$$

where $a(r, z)$ is an even function of z and with an odd toroidal field $B_\phi(r, -z) = -B_\phi(r, r)$. The flux function a is related to the toroidal component of the potential vector ($a = rA_\phi$) and $a(r, z) = constant$ describes a surface of constant vertical magnetic flux Φ,

$$\Phi = \int_S \vec{B} \cdot d\vec{S} = 2\pi a(r, z) \ . \tag{2.27}$$

The magnetic field distribution in the disc as well as the total amount of flux are unknown and must therefore be prescribed.

(iii) Steady-state : all astrophysical jets display proper motions and/or emission nodules, showing that they are either prone to some instabilities or that ejection is an intermittent process. However, the time scales involved in all objects are always much larger than the dynamical time scale of the underlying accretion disc. Therefore, a steady state approach is appropriate[3].

(iv) Transport coefficients : if we use a normal (collisional) value for ν, we find that the ratio of advection to diffusion in (2.25), measured by the magnetic Reynolds number

$$\mathcal{R}_m \sim \frac{LU}{\nu} \ , \tag{2.28}$$

is always much larger than unity inside both the disc and the jets. This is the limit of ideal MHD where plasma and magnetic fields are "frozen in". Jets are therefore described with ideal MHD ($\eta = 0$). Within this framework, the stronger (initially the magnetic field) carries the weaker (ejected disc plasma) along with it. But inside the disc, gravitation is the dominant energy source and the plasma drags and winds up the field lines. Such a situation cannot be maintained for very long. Instabilities of different kind will certainly be triggered leading to some kind of saturated, turbulent, disc state (eg. tearing mode instabilities, or magneto-rotational instability, Balbus & Hawley 1991).

In turbulent media, all transport effects are enhanced, leading to anomalous transport coefficients. These coefficients are the magnetic diffusivity ν_m and resistivity η_m, but also the viscosity ν_v (associated with the transport of momentum) and thermal conductivity κ_T (associated with the heat flux). Providing the expressions of these anomalous coefficients requires a theory of MHD turbulence inside accretion discs. Having no theory, we will use simple prescriptions, like the alpha prescription used by Shakura & Sunyaev (1973). In particular, because of the dominant keplerian motion in discs, we allow for a possible anisotropy of the magnetic diffusivity. Namely, we use two different turbulent diffusivities : ν_m (related to the diffusion in the (r, z) plane) and ν'_m (related to the diffusion in the ϕ direction).

Since stationary discs must be turbulent, all fields (eg. velocity, magnetic field) must be understood now in some time average sense.

(v) Non-relativistic MHD framework : in YSOs, matter remains always non-relativistic but there is something more about it. Indeed, magnetic field lines are anchored in an rotating accretion disc. Hence, if a field line of angular velocity Ω_* opens a lot, there is a cylindrical distance such

[3]Note that this conclusion holds even in microquasars. In GRS 1915+105 the duration of an ejection event is around 10^3 sec only, but the disc dynamical time scale is around 1 msec, ie. 10^{-6} times smaller. See however Tagger & Pellat (1999) and Tagger et al. (2004) and for an alternative view on this topic.

that its linear velocity reaches the speed of light, defining a "light cylinder" $R_L = c/\Omega_*$. Now, if one imposes ideal MHD regime along the jet, ie. $\vec{E} = -\vec{u} \wedge \vec{B} = -\Omega_* r \vec{e_\phi} \wedge \vec{B_p}$, we see that the displacement current is no longer negligible at the light cylinder : propagation effects become relevant and one must take into account a local non-zero electric charge ρ_* (provided by the Goldreich-Julian charge $\nabla \cdot \vec{E} = \rho_*/\varepsilon_o$). As a consequence, the plasma feels an additional electric force $\rho_* \vec{E}$, even if the bulk velocity of the flow is non relativistic (eg. Breitmoser & Camenzind 2000) !

But remember that this extra force and its corresponding "light cylinder" arose because of the *assumption* of ideal MHD. In fact, taking into account a local charge density probably imposes to also treat the non-ideal contributions (see Eq. 2.21). Nobody provided yet a self-consistent calculation. We just assume here that any charge accumulation would be quickly canceled (no dynamical relevance of the light cylinder).

Set of MHD equations

We use the following set of MHD equations :

Mass conservation

$$\nabla \cdot \rho \vec{u} = 0 \tag{2.29}$$

Momentum conservation

$$\rho \vec{u} \cdot \nabla \vec{u} = -\nabla P - \rho \nabla \Phi_G + \vec{J} \wedge \vec{B} + \nabla \cdot \mathsf{T} \tag{2.30}$$

where $\mu_o \vec{J} = \nabla \wedge \vec{B}$ is the current density and T the turbulent stress tensorm which is related to the turbulent viscosity ν_v (Shakura & Sunyaev 1973).

Ohm's law and **toroidal field induction**[4]

$$\eta_m \vec{J_\phi} = \vec{u_p} \wedge \vec{B_p} \tag{2.31}$$

$$\nabla \cdot \left(\frac{\nu'_m}{r^2} \nabla r B_\phi\right) = \nabla \cdot \frac{1}{r}(B_\phi \vec{u_p} - \vec{B_p} \Omega r) \tag{2.32}$$

where $\eta_m = \mu_o \nu_m$ and $\eta'_m = \mu_o \nu'_m$ are the anomalous resistivities.

Perfect gas law

$$P = \rho \frac{k_B}{\mu m_p} T \tag{2.33}$$

where m_p is the proton mass and μ a generalized "mean molecular weight".

Energy equation

As seen previously, the exact energy equation (2.22) involves various physical mechanisms. Its explicit form is

$$\nabla \cdot (U \vec{u_p} + \vec{S_{rad}} + \vec{q_{turb}}) = -P \nabla \cdot \vec{u_p} + \eta_m J_\phi^2 + \eta'_m J_p^2 + \eta_v |r \nabla \Omega|^2 \tag{2.34}$$

[4] Obtained from Eq. (2.25) and after some algebra (remember that $E_\phi = 0$).

where $\eta_v = \rho\nu_v$, U is the internal specific energy, $\vec{S}_{rad} = -\frac{c}{\kappa\rho}\nabla P_{rad}$ is the radiative energy flux (κ is the Rosseland mean opacity of the plasma, P_{rad} the radiation pressure) and $\vec{q}_{turb}$ the unknown turbulent energy flux. This flux of energy arises from turbulent motions and provides both a local cooling Λ_{turb} and heating Γ_{turb}. Indeed, using a kinetic description and allowing for fluctuations in the plasma velocity and magnetic field, it is possible to show that all energetic effects associated with these fluctuations cannot be reduced to only anomalous Joule and viscous heating terms. Therefore, a consistent treatment of turbulence imposes to take into account $\vec{q}_{turb}$ (see early paper of Shakura et al. 1978). But how to do it ? Moreover, the radiative flux depends on the local opacity κ of the plasma, which varies both radially and vertically inside the disc. Besides, the expression of the radiative pressure P_{rad} is known only in optically thick media ($P_{rad} = aT^4$), while the disc can be already optically thin at the disc midplane.

Thus, it seems that a realistic treatment of the energy equation is still out of range. As a first step to minimize its impact on the whole structure, we will use a polytropic equation

$$P = K\rho^{\Gamma} \ , \tag{2.35}$$

where the polytropic index Γ can be set to vary between 1 (isothermal case) and $\gamma = \frac{5}{3}$ (adiabatic case) for a monoatomic gas. Here K can be allowed to vary radially but remains constant along each field line. In section 2.5.3, we will turn on our attention to thermal effects and use therefore a more appropriate form of the energy equation.

Using the above set of MHD equations to describe astrophysical discs and jets would normally require consistency checks, at least *a posteriori*. If one fluid MHD seems justified inside the inner regions of accretion discs, it may well not be anymore the case along the jet (huge fall in density). In particular non-ideal effects are most probably starting to play a role in Ohm's law (ambipolar diffusion or even Hall terms), allowing matter to slowly drift across field lines. This may have important dynamical effects downstream the jets. To clearly settle this question, the full thermodynamics of the plasma including its ionization state should be self-consistently solved along the jet.

2.2.4 Critical points in stationary flows

In the real world, everything is time dependent. Imagine matter expelled from the disc without the required energy : it will fall down, thereby modifying the conditions of ejection. A steady state is eventually reached after a time related to the nature of the waves travelling upstream and providing to the disc information on what's going on further up.

The adjustment of a MAES corresponds to the phenomenon of impedance matching. As we saw, this matching relates the accretion rate to the dissipative effects in the global electric circuit. In practice, this means that the resolution of stationary flows requires to take into account, in some way, all time-dependent feedback mechanisms. This is done by requiring that, once a steady-state is achieved, no information (ie. no waves) can propagate upstream, from infinity (in the z-direction) to the accretion disc. There is only one way to do it. Matter must flow faster than any wave, leaving the disc causally disconnected from its surroundings.

The Parker wind

Let us first look at the simple model of a spherically symmetric, isothermal, hydrodynamic flow. Such a model was first proposed by Parker (1958) to explain the solar wind. In spherical coordinates, mass conservation and momentum conservation write

$$\frac{du}{u}+\frac{d\rho}{\rho}+2\frac{dr}{r} = 0 \tag{2.36}$$

$$u\frac{du}{dr}+\frac{1}{\rho}\frac{dP}{dr}+\frac{GM}{r^2} = 0 \tag{2.37}$$

where gas pressure is $P=\rho C_s^2$, the sound speed C_s being a constant. In such a simple system is hidden a singularity. Indeed, after differentiation one gets

$$(C_s^2-u^2)\frac{d\ln\rho}{dr} = 2\frac{u^2}{r}-\frac{GM}{r^2} \tag{2.38}$$

$$(C_s^2-u^2)\frac{d\ln u}{dr} = -2\frac{C_s^2}{r}+\frac{GM}{r^2} \tag{2.39}$$

showing that the system is singular at $r=r_s$, where $u=C_s$. In order to obtain a stationary solution, one must then impose the regularity condition which is

$$r_s=\frac{GM}{2C_s^2} \tag{2.40}$$

In practice, fixing the distance of the sonic point imposes the value of one free parameter (eg. the initial velocity or density). Only the trans-sonic solution is stationary.

Critical points of a MAES

In a magnetized medium, there are several waves able to transport information, related to the different restoring forces. In a MAES, the Lorentz

force couples with the plasma pressure gradient leading to three different MHD waves :

– the Alfvén wave (A), causing only magnetic disturbances along the unperturbed magnetic field B_o and of phase velocity

$$V_A = \frac{B_o}{\sqrt{\mu_o \rho}}$$

– two magnetosonic waves, the slow (SM) and the fast (FM), involving both magnetic disturbances and plasma compression (or rarefaction), of phase velocity

$$V^2_{SM,FM} = \frac{1}{2}\left(V_A^2 + C_s^2 \mp \sqrt{(V_A^2 + C_S^2)^2 - 4V_A^2 C_s^2 \cos^2\theta}\right)$$

where θ is the angle between the unperturbed field B_o and the direction of propagation of the wave (the disturbance).

In ideal MHD regime (in the jets), these three waves can freely propagate. This provides three singularities along *each* magnetic surface, whenever the plasma velocity equals one of these phase speeds. Thus, three regularity conditions must be specified per magnetic surface.

Inside the turbulent accretion disc it is another story. There, the high level of turbulence maintains large magnetic diffusivities and viscosity. As a result, MHD waves are strongly damped and the number of singularities really present is not so clear. Within the alpha prescription of accretion discs (Shakura & Sunyaev 1973), viscosity appears only in the azimuthal equation of motion (angular momentum conservation). The presence of viscosity there "damps" the acoustic waves and there is no singularity related to this motion (although keplerian rotation is supersonic). Conversely, there is no viscosity in the poloidal (radial and vertical) equations of motion : a singularity can therefore appear there, related to pure acoustic waves. As a consequence, in principle, it may be necessary to impose a regularity condition with respect to the poloidal accretion flow itself, if it becomes supersonic.

2.3 Magnetized jets

2.3.1 Commonly used equations

As said previously, jets are in ideal MHD regime, namely $\nu_v = \nu_m = \nu'_m = 0$. In this regime, mass and flux conservations combined with Ohm's law (2.31) provide

$$\vec{u}_p = \frac{\eta(a)}{\mu_o \rho}\vec{B}_p \tag{2.41}$$

where $\eta(a) = \sqrt{\mu_o \rho_A}$ is a constant along a magnetic surface[5] and ρ_A is the density at the Alfvén point, where the poloidal velocity u_p reaches the poloidal Alfvén velocity V_{Ap}. The induction equation (2.32) becomes

$$\Omega_*(a) = \Omega - \eta \frac{B_\phi}{\mu_o \rho r} \ , \tag{2.42}$$

where $\Omega_*(a)$ is the rotation rate of a magnetic surface (imposed by the disc, thus very close to the keplerian value). Note that despite the frozen in situation, jet plasma flows along a magnetic surface with a total velocity $\vec{u} = (\eta/\mu_o\rho)\vec{B} + \Omega_* r \vec{e_\phi}$ which is **not** parallel to the total magnetic field $\vec{B}$. This is possible because field lines rotate faster than the ejected plasma. If the disc is rotating counter-clockwise, the field lines will be trailing spirals ($\Omega_* > \Omega$, ie. $B_\phi < 0$ with $B_z > 0$), while ejected plasma will rotate in the same direction as in the disc. Magnetic field lines and plasma stremlines are thus two helices of different twist. Jet angular momentum conservation simply writes

$$\Omega_* r_A^2 = \Omega r^2 - \frac{r B_\phi}{\eta} \tag{2.43}$$

where r_A is the Alfvén radius. Above the disc, the turbulent torque vanishes and only remains a magnetic accelerating torque. The first term on rhs is the specific angular momentum carried by the ejected plasma whereas the last term can be understood as the angular momentum stored in the magnetic field. The total specific angular momentum $L(a) = \Omega_* r_A^2$ is an MHD invariant. The Alfvén radius r_A can be interpretated as a magnetic lever arm, braking down the disc. The larger the ratio r_A/r_o, the larger the magnetic torque acting on the disc at the radius r_o.

Hereafter, we focus only on adiabatic jets (for which thermal effects can still be non negligible). Usually, instead of using the other two components of the momentum conservation equation, one uses the Bernoulli equation (obtained by projecting Eq. (2.30) along the poloidal direction, ie. $\vec{B_p}$) and the transverse field or Grad-Shafranov equation (obtained, after quite a lot of algebra, by projecting Eq. (2.30) in the direction perpendicular to a magnetic surface, ie. ∇a). For a jet of adiabatic index γ, Bernoulli equation writes

$$E(a) = \frac{u^2}{2} + H + \Phi_G - \Omega_* r \frac{B_\phi}{\sqrt{\mu_o \rho_A}} \tag{2.44}$$

where u is the total plasma velocity and $H = (\gamma/\gamma{-}1)P/\rho$ is the gas enthalpy. This equation describes the acceleration of matter along a poloidal magnetic

[5] Any quantity Q verifying $\vec{B}_p \cdot \nabla Q = 0$ is a constant along a poloidal magnetic field line, hence an MHD invariant on the corresponding magnetic surface.

surface, namely the conversion of magnetic energy and enthalpy into ordered kinetic energy. Grad-Shafranov equation of an adiabatic jet is

$$\nabla \cdot (m^2-1)\frac{\nabla a}{\mu_o r^2} = \rho\left\{\frac{dE}{da} - \Omega\frac{d\Omega_* r_A^2}{da} + (\Omega r^2 - \Omega_* r_A^2)\frac{d\Omega_*}{da} - \frac{C_s^2}{\gamma(\gamma-1)}\frac{d\ln K}{da}\right\} + \frac{B_\phi^2 + m^2 B_p^2}{\mu_o}\frac{d\ln\eta}{da} \quad (2.45)$$

where $m^2 \equiv u_p^2/V_{Ap}^2$ is the Alfvénic Mach number and $C_s^2 = \gamma k_B T/\mu m_p$ is the jet sound speed. This awful equation provides the transverse equilibrium (ie. the degree of collimation) of a magnetic surface. A simpler-to-use and **equivalent** version of this equation is

$$(1-m^2)\frac{B_p^2}{\mu_o \mathcal{R}} - \nabla_\perp\left(P + \frac{B^2}{2\mu_o}\right) - \rho\nabla_\perp\Phi_G + (\rho\Omega^2 r - \frac{B_\phi^2}{\mu_o r})\nabla_\perp r = 0 \quad (2.46)$$

where $\nabla_\perp \equiv \nabla a \cdot \nabla/|\nabla a|$ provides the gradient of a quantity perpendicular to a magnetic surface ($\nabla_\perp Q < 0$ for a quantity Q decreasing with increasing magnetic flux) and $\mathcal{R}$, defined by

$$\frac{1}{\mathcal{R}} \equiv \frac{\nabla a}{|\nabla a|} \cdot \frac{(\vec{B}_p \cdot \nabla)\vec{B}_p}{B_p^2} \ , \quad (2.47)$$

is the local curvature radius of a particular magnetic surface. When $\mathcal{R} > 0$, the surface is bent outwardly while for $\mathcal{R} < 0$, it bends inwardly. The first term in Eq.(2.46) describes the reaction to the other forces of both magnetic tension due to the magnetic surface (with the sign of the curvature radius) and inertia of matter flowing along it (hence with opposite sign). The other forces are the total pressure gradient, gravity (which acts to close the surfaces and deccelerate the flow, but whose effect is already negligible at the Alfvén surface), and the centrifugal outward effect competing with the inwards hoop-stress due to the toroidal field.

To summarize, an astrophysical jet is a bunch of axisymmetric magnetic surfaces $a(r,z) = Const.$, nested one around the other at different anchoring radii r_o. The magnetic flux distribution $a(r_o)$ is unknown and is therefore prescribed, whereas the shape $r(z)$ of the magnetic surface is self-consistently calculated. Each magnetic surface is characterized by 5 MHD invariants :

- $\eta(a)$, ratio of ejected mass flux to magnetic flux ;
- $\Omega_*(a)$, the rotation rate of the magnetic surface ;
- $L(a) = \Omega_* r_A^2$, the total specific angular momentum transported ;
- $E(a)$, the total specific energy carried away ;
- $K(a)$, related to the specific entropy $S(a)$.

A magnetized jet is described by 8 variables : density ρ, velocity $\vec{u}$, magnetic field $\vec{B}$ (flux function a and toroidal field B_ϕ), pressure P and temperature T. There are 8 equations allowing us to solve the complete problem : (2.26), (2.33), (2.35), (2.41), (2.42), (2.43), (2.44) and (2.45) or its more physically meaningful version (2.46). Since the ejected plasma must become super Fast-Magnetosonic, 3 regularity conditions have to be imposed, leaving the problem with 5 free boundary conditions (at each radius r_o). Studies of disc-driven jets usually take the disc surface as a "platform" where some boundary conditions are freely imposed. One such condition is a keplerian rotation rate of the ejected material, $\Omega_o = \Omega_K(r_o) = \sqrt{GM/r_o^3}$. Another is that jets are "cold" (negligible enthalpy, $K(a) = 0$) or choose an arbitrary distribution $K(a)$. In both cases, it leaves the problem with only 3 **free and independent** boundary conditions that must be specified at each radius[6].

Magnetized jets are such complicated objects that only gross properties are known. For example, we know that a non-vanishing asymptotic current will produce a self-confinement of *some* field lines (Heyvaerts & Norman 1989, 2003). But the exact proportion of collimated field lines depends on "details" (transverse gradients of inner properties, outer pressure). The distance at which jets become collimated, the jet radius and opening angle, the velocity and density transverse distributions still remain to be found in full generality. This is the reason why there are so many different works on jet dynamics and why each authors use their own "relevant" parameters. Following Blandford & Payne (1982), we introduce the following jet parameters

$$\begin{aligned} \lambda &= \frac{\Omega_* r_A^2}{\Omega_o r_o^2} \simeq \frac{r_A^2}{r_o^2} \simeq 1 - \frac{B_\phi^+}{\eta \Omega_o r_o} \\ \kappa &= \eta \frac{\Omega_o r_o}{B_o} \simeq \frac{\mu_o \Omega_o r_o}{B_o^2} \rho^+ u_z^+ \end{aligned} \tag{2.48}$$

The index "o" refers to quantities evaluated at the disc midplane, "+" at the disc surface and "A" at the Alfvén point. The first parameter, λ, is a measure of the magnetic lever arm that brakes down the disc while κ measures the ejected mass flux. Another parameter is usually introduced, related somehow to the jet asymptotic behaviour. We use

$$\omega_A = \frac{\Omega_* r_A}{V_{Ap,A}} \simeq \kappa \lambda^{1/2} \frac{B_o}{B_{p,A}} \tag{2.49}$$

[6]In numerical MHD computations, one usually prescribes the density $\rho^+(r_o)$, vertical velocity $u_z^+(r_o)$ and magnetic field $B_z^+(r_o)$ distributions (eg. Ouyed & Pudritz 1997, 1999, Krasnopolsky et al. 1999). In those self-similar jet studies where only the Alfvén point has been crossed, 4 (if $K(a) = 0$, Blandford & Payne 1982) of 5 (if $K(a) \neq 0$, Contopoulous & Lovelace 1994) variables remain free and independent (ρ^+, u_z^+, B_z^+, B_ϕ^+ and P^+).

which measures the ratio of the rotational velocity to the poloidal jet velocity at the Alfvén point. Such a parameter characterises the magnetic rotator : cold jets require $\omega_A > 1$ to become trans-Alfvénic (Pelletier & Pudritz 1992, Ferreira 1997, Lery et al. 1999). Note also that its value depends on pure geometrical effects, namely the way the magnetic surface opens. As a consequence, spherical expansion of field lines such as in Shu et al (1994) X-wind model, is probably a special case leading to particular relations between jet asymptotic behaviour and its source.

2.3.2 Some aspects of cold jets physics

Energetic requirements

It is quite reasonable to assume that the magnetic energy density in the disc is much smaller than the gravitational energy density. As a consequence, the rotation of the disc drags the magnetic field lines which become then twisted. This conversion of mechanical to magnetic energy in the disc gives rise to an outward poloidal MHD Poynting flux

$$\vec{S}_{MHD,p} = \frac{\vec{E} \times \vec{B}_\phi}{\mu_o} = -\Omega_* r B_\phi \frac{\vec{B}_p}{\mu_o} \tag{2.50}$$

which feeds the jets and appears as the magnetic term in the Bernoulli integral (2.44). Another source of energy for the jet could be the enthalpy H (built-in inside the disc and advected along by the ejected flow) or another local source of heating $\mathcal{Q}$ (eg. coronal heating). We are mainly interested here in "cold" jets, where those two terms are negligible (see Sect. 2.5.3). Bernoulli equation can be rewritten as

$$E(a) = \frac{u_p^2}{2} \; + \; \Phi_{eff} \; + \; H \tag{2.51}$$

where the effective potential is $\Phi_{eff} = \Phi_G - \frac{1-g^2}{2}\Omega_*^2 r^2$ with $\Omega = \Omega_*(1-g)$ and $\Omega_* \simeq \Omega_o$. The function g is much smaller than unity at the disc surface then increases along the jet (if the jet widens a lot, $g \to 1$). Starting from a point located at the disc surface $(r_o, z = 0)$, matter follows along a magnetic surface and must move to another point $(r_o + \delta r_o, z)$. This can be done only if a positive poloidal velocity is indeed developed. Making a Taylor expansion of Φ_{eff}, one gets $\frac{u_p^2}{2} \simeq H_o - H + \frac{\Omega_o^2}{2}(3\delta r_o^2 - z^2) > 0$, which translates into the condition

$$\tan\theta = \frac{z}{\delta r_o} < \sqrt{3}\left(1 + \frac{2}{3}\frac{H_o - H}{\Omega_o^2 \delta r_o^2}\right)^{1/2} \quad . \tag{2.52}$$

Thus, cold jets (negligible enthalpy) require field lines bent by more than 30^o with respect to the vertical axis at the disc surface (Blandford & Payne 1982). The presence of a significant enthalpy (H_o large) is obviously required if this condition is not satisfied. Bernoulli equation (2.44) gives a total energy feeding a **cold** jet

$$E(a) = \frac{\Omega_o^2 r_o^2}{2} - \Omega_o^2 r_o^2 + \Omega_*(\Omega_* r_A^2 - \Omega_o r_o^2) = \frac{\Omega_o^2 r_o^2}{2}(2\lambda - 3) \tag{2.53}$$

which is directly controlled by the magnetic lever arm λ. Cold, super-FM jets require therefore $\lambda > 3/2$. If all available energy is converted into kinetic energy, ejected plasma reaches an asymptotic poloidal velocity $u_\infty(a) = \sqrt{2E(a)} = \Omega_o r_o \sqrt{2\lambda - 3} \simeq \Omega_o r_A$ (the latter valid only if $\lambda \gg 3/2$).

Relevant forces and current distributions

So, rotation of open field lines produces a shear ($B_\phi^+ < 0$) that results in an outward flux of energy. Once matter is loaded onto these field lines, it will be flung out whenever there are forces overcoming the gravitational attraction. Since matter flows along magnetic surfaces, one must look at the projection of all forces along these surfaces (fig.2.2). We obtain for the Lorentz force,

$$\begin{aligned} F_\phi &= \frac{B_p}{2\pi r}\nabla_\parallel I \\ F_\parallel &= -\frac{B_\phi}{2\pi r}\nabla_\parallel I \end{aligned} \tag{2.54}$$

where $\nabla_\parallel = \vec{\nabla}\cdot\vec{B}_p/B_p$ and $I = 2\pi r B_\phi/\mu_o$ is the total poloidal current flowing inside the magnetic surface. Hence, jets are magnetically-driven whenever $\nabla_\parallel I > 0$ is fulfilled, namely when current is leaking through this surface. This quite obscure condition describes the fact that magnetic energy is being converted into kinetic energy : the field lines accelerate matter **both** azimuthaly ($F_\phi > 0$) and along the magnetic surface ($F_\parallel > 0$). The difference with the Barlow wheel lies in the possibility to convert magnetic energy into jet (bulk) kinetic energy.

The jet transverse equilibrium depends on the subtle interplay between several forces (see Eq. (2.46)). The transverse projection of the magnetic force, namely

$$F_\perp = B_p J_\phi - \frac{B_\phi}{2\pi r}\nabla_\perp I \tag{2.55}$$

where $\nabla_\perp \equiv (\nabla a \cdot \nabla)/|\nabla a|$, shows that it depends on the transverse current distribution. Thus, the degree of jet collimation (as well as plasma acceleration) depends on the overall electric current circuit. Any bias introduced

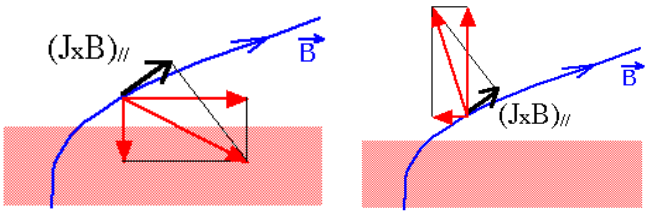

FIG. 2.2 – Magnetic poloidal acceleration arises whenever the projection of the Lorentz force on a poloidal field line becomes positive. This can be achieved in two ways, either with a downward vertical magnetic compression or a strong outward pressure force due to the toroidal field. The former leads to a small ejection efficiency and has current lines coming out of the disc surface ($J_z^+ > 0$) and entering it at the inner radius. The latter has a strong ejection efficiency with the current entering the disc at its surfaces ($J_z^+ < 0$). Only the former configuration reaches a steady state (Ferreira 1997). It corresponds best to the so-called "magneto-centrifugal" driving whereas the second configuration corresponds to a magnetic pressure driving by the toroidal magnetic field.

on this circuit can produce an artificial force and modify diagnostics on jet collimation.

Eventually matter becomes no longer magnetically accelerated and $\nabla_{\parallel} I = 0$ is satisfied. This implies two possible asymptotic current distributions. If jets are force-free (ie. $\vec{J}_p$ and $\vec{B}_p$ parallel), then there is a non-vanishing asymptotic current providing a self-collimating pinch (and one must worry about how the electric circuit is closed). Or, jets become asymptotically current-free ($I_\infty = 0$) and another cause must then be responsible for their collimation beyond this point (either inertial or external pressure confinement). This last alternative has something appealing for magnetic fields would then have a major influence only at the jet basis, becoming dynamically negligible asymptotically.

2.3.3 Numerical simulations

What can be learned from them ? There have been a lot of numerical studies of MHD jet propagation and their associated instabilities. Here, I focus only on those addressing the problem of jet formation from accretion discs. Although some attempts have been made to model accretion discs driving jets, difficulties are such that nothing realistic has been obtained yet (Shibata & Uchida 1985, Stone & Norman 1994, Kudoh et al. 1998). Ejection

is indeed observed, but no one can tell whether these events are just transients or if they indeed represent some realistic situation[7].

Another philosophy is to treat the disc as a boundary condition and, starting from an (almost) arbitrary initial condition, wait until the system converges towards a stationary flow (Ustyugova et al. 1999, 2000, Ouyed & Pudritz 1997, 1999, Krasnopolsky et al. 1999). Now, it is of no wonder that jets are indeed obtained with these simulations. Matter, forced to flow along open magnetic field lines, is continuously injected (at a rate $\rho^+ u_z^+$) at the bottom of the computational box. As a response, the field lines twist (ie. B_ϕ increases) until there is enough magnetic energy to propell it. If the code is robust enough, a steady-state situation is eventually reached. Ouyed & Pudritz (1997) found a parameter region where unsteady solutions are produced, with a "knot generator" whose location seems to remain constant in time. Their results may be related to the characteristic recollimation configuration featured by self-similar solutions (Blandford & Payne 1982, Contopoulos & Lovelace 1994, Ferreira 1997).

Nevertheless, since the time step for computation depends on the faster waves (Courant condition) whose phase speed varies like $\rho^{-1/2}$, it appears that no current MHD code can cope with tiny mass fluxes. Thus, code convergence itself introduces a bias in the mass flux of numerical jets. These are always very "heavy", with a magnetic lever arm r_A/r_o not reaching 4 (Ouyed & Pudritz 1999, Krasnopolsky et al. 1999, Ustyugova et al. 1999) while cold self-similar studies obtained much larger values (up to 100). This is not a limitation imposed by physics but of computers and will certainly be overcome in the future. Note also that boundary conditions imposed at the box, as well as the shape of the computational domain, can introduce artificial forces leading to unsteady jets or spurious collimation (see the nice paper of Ustyugova et al. 1999).

However, these numerical experiments provide a fantastic and powerful means to investigate the question of jet collimation and stability as a function of the free distributions B_z, ρ and v_z (see Ouyed et al 2003, Pudritz et al 2006). Anyway, the following crucial question remains to be addressed : **how (and how much) matter is loaded into the field lines ?** Or another way to put it : how is matter steadily deflected from its radial motion (accretion) to a vertical one (ejection) ? To answer this question one must treat the accretion disc in a self-consistent way.

[7]This is not anymore the case now. In 2002 and 2004 Casse & Keppens obtained the first quasi stationary simulations of a MAES using the VAC code. Zanni et al (2004, 2007) recovered their results using the AMR FLASH code. Both simulations confirmed the general requirements as exposed in Ferreira & Pelletier (1995) and Ferreira (1997).

2.4 Jet emitting discs

2.4.1 Physical processes in quasi-keplerian discs

Turbulent, keplerian discs

As said previously, we focus our study on quasi-keplerian accretion discs. Such a restriction imposes negligible radial plasma pressure gradient and magnetic tension. We define the local vertical scale height as $P_o = \rho_o \Omega_K^2 h^2$ where P_o is the total (gas+radiation) plasma pressure and $h(r)$ the disc half thickness (namely, the vertical pressure length scale). Looking at the disc radial equilibrium, a keplerian rotation rate is indeed obtained whenever the disc aspect ratio

$$\varepsilon = \frac{h(r)}{r} \tag{2.56}$$

is smaller than unity. Hereafter, we use $\varepsilon < 1$ as a free parameter and we will check *a posteriori* the thin disc approximation (Sect. 2.5.4).

Steady accretion requires a turbulent magnetic diffusivity for matter must cross field lines while accreting and rotating. Since rotation is much faster than accretion, there must be a higher dissipation of toroidal field than poloidal one. *A priori*, this implies a possible anisotropy of the magnetic diffusivities associated with these two directions, poloidal ν_m and toroidal ν'_m. Besides, such a turbulence might also provide a radial transport of angular momentum, hence an anomalous viscosity ν_v. To summary, three anomalous transport coefficients are necessary to describe a stationary MAES. We will use the following dimensionless parameters defined at the disc midplane :

$$\begin{aligned} \alpha_m &= \frac{\nu_m}{v_A h} && \text{level of turbulence} \\ \chi_m &= \frac{\nu_m}{\nu'_m} && \text{degree of anisotropy} \\ \mathcal{P}_m &= \frac{\nu_v}{\nu_m} && \text{magnetic Prandtl number} \end{aligned} \tag{2.57}$$

where $v_A = B_o/\sqrt{\mu_o \rho_o}$ is the Alfvén speed. Our conventional view of 3D turbulence would translate into $\alpha_m < 1$, $\chi_m \sim 1$ and $\mathcal{P}_m \sim 1$. But as stated before, the amount of current dissipation may be much higher in the toroidal direction, leading to $\chi_m \ll 1$. Moreover, it is not obvious that α_m must necessarily be much smaller than unity. Indeed, stationarity requires that the time scale for a magnetic perturbation to propagate in the vertical direction, h/v_A, is longer than the dissipation time scale, h^2/ν_m. This roughly translates into $\alpha_m > 1$. Thus, we must be cautious and will freely scan the parameter space defined by these turbulence parameters.

How is accretion achieved ?

The disc being turbulent, accretion of matter bends the poloidal field lines whose steady configuration is provided by Ohm's law (2.31). At the disc midplane, this equation provides

$$\mathcal{R}_m \equiv \frac{r u_o}{\nu_m} = \left.\frac{\mu_o r J_\phi}{B_z}\right|_{z=0} \sim \frac{l^2}{r^2} \tag{2.58}$$

where $\mathcal{R}_m$ is the magnetic Reynolds number related to the radial motion u_o and $l(r)$ is the characteristic scale height of the magnetic flux variation. Once the disc turbulence properties are given, we just need to know the accretion velocity u_o. This is provided by the angular momentum equation, namely

$$\rho \frac{\vec{u}_p}{r} \cdot \nabla \Omega r^2 = F_\phi + (\nabla \cdot \mathsf{T}) \cdot \vec{e}_\phi \tag{2.59}$$

where F_ϕ is the magnetic torque due to the large scale magnetic field (jet torque) and $(\nabla \cdot \mathsf{T}) \cdot \vec{e}_\phi = \frac{1}{r^2}\frac{\partial}{\partial r}\rho\nu_v r^3 \frac{\partial \Omega}{\partial r}$ is the "viscous"-like torque with the alpha turbulent viscosity ν_v (Shakura & Sunyaev 1973), possibly due to the magneto-rotational instability (see Balbus 2003 and references therein). Such an equation can be put into the following conservative form

$$\nabla \cdot \left[\rho \Omega r^2 \vec{u}_p \; - \; \frac{r B_\phi}{\mu_o} \vec{B}_p \; - \; r \vec{T}_v \right] = 0 \tag{2.60}$$

where $r(\nabla \cdot \mathsf{T}) \cdot \vec{e}_\phi = \nabla \cdot r\vec{T}_v$. Although modelling the jet torque is quite straightforward, it is not the case of the turbulent torque $\vec{T}_v$ and we use a prescription analogous to Shakura & Sunyaev (1973). Defining

$$\Lambda = \left| \frac{\text{jet torque}}{\text{turbulent torque}} \right|_{z=0} \tag{2.61}$$

the disc angular momentum conservation becomes at the disc midplane

$$1 + \Lambda \simeq \mathcal{R}_m \left(\frac{\nu_m}{\nu_v} \right) = \frac{\mathcal{R}_m}{\mathcal{P}_m} \tag{2.62}$$

Taking the conventional value $\mathcal{P}_m \sim 1$, one sees that a "standard" accretion disc, which is dominated by the viscous torque ($\Lambda \ll 1$) requires straigth poloidal field lines ($\mathcal{R}_m \sim 1$, Heyvaerts et al. 1996). On the contrary, cold jets carrying away all disc angular momentum ($\Lambda \gg 1$) are produced with bent magnetic surfaces so that $\mathcal{R}_m \sim \Lambda \sim \varepsilon^{-1}$ (Ferreira & Pelletier 1995).

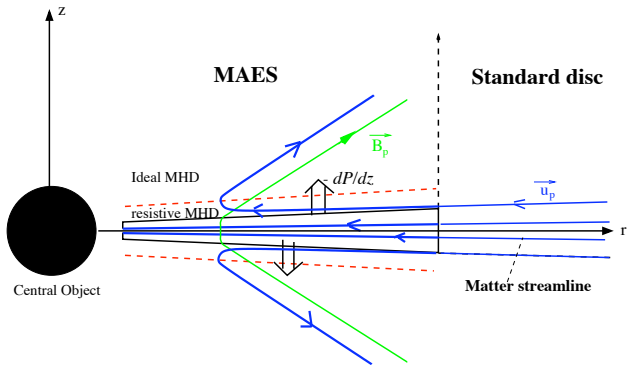

FIG. 2.3 – Sketch of a Magnetized Accretion Ejection Structure (Courtesy of Fabien Casse).

How is matter defleted from accretion ?

The poloidal components of the momentum conservation equation write

$$\left(\vec{u}_p \cdot \vec{\nabla}\right) u_r = (\Omega^2 - \Omega_K^2) r + \frac{F_r}{\rho} - \frac{1}{\rho}\frac{\partial P}{\partial r} \tag{2.63}$$

$$\left(\vec{u}_p \cdot \vec{\nabla}\right) u_z \simeq -\frac{1}{\rho}\frac{\partial P}{\partial z} - \Omega_K^2 z - \frac{1}{\rho}\frac{\partial}{\partial z}\frac{B_r^2 + B_\phi^2}{2\mu_o} \tag{2.64}$$

At the disc midplane, a total (magnetic + viscous) negative torque provides an angular velocity slightly smaller than the keplerian one $\Omega_K = \sqrt{GM/r_o^3}$, thereby producing an accretion motion ($u_r < 0$). But at the disc surface, one gets an outwardly directed flow ($u_r^+ > 0$) because both the magnetic tension F_r (whose effect is enhanced by the fall in density) and the centrifugal force overcome gravitation ($\Omega^+ > \Omega_K$). Note that jets are magnetically-driven, the centrifugal force resulting directly from the positive magnetic torque ($F_\phi^+ > 0$). This can be understood with a simple geometrical argument : matter has been loaded onto field lines that are anchored at inner radii and are thus rotating faster (see fig. 2.3).

But again, we assumed that matter is being loaded from the underlying layers with $u_z^+ > 0$. The physical mechanism is hidden in Eq. (2.64) : the only force that can *always* counteract both gravity and magnetic compression is the plasma pressure gradient (Ferreira & Pelletier 1995). Inside the disc, a quasi-MHS equilibrium is achieved, with matter slowly falling down ($u_z < 0$) while accreting. However, plasma coming from an outer disc region eventually reaches the upper layers at inner radii. There, the plasma pres-

sure gradient slightly wins and gently lifts matter up ($u_z^+ > 0$), at an altitude which depends on the local disc energetics.

How is steady ejection obtained ?

Is ejection unavoidable once all above[8] ingredients are met ? The answer is "yes", but **steady** ejection requires another condition.

While accretion is characterized by a negative azimuthal component of the Lorentz force F_ϕ, magnetic acceleration occurring in jets requires a positive F_ϕ. Since $F_\phi = J_z B_r - J_r B_z$, the transition between these two situations depends mainly on the vertical profile of the radial current $J_r \equiv -\mu_o^{-1} \partial B_\phi / \partial z$, that is, on the rate of change of the magnetic shear with altitude. In order to switch from accretion to ejection, J_r must vertically decrease on a disc scale height. This crucial issue is controlled by Eq. (2.32), that provides

$$\eta'_m J_r \simeq \eta'_o J_o \ + \ r \int_0^z dz \vec{B_p} \cdot \nabla \Omega \ - \ B_\phi u_z \tag{2.65}$$

The first term on the rhs describes the current due to the electromotive force, the second is the effect of the disc differential rotation and the third is the advection effect, only relevant at the disc surface layers. Thus, the vertical profile of J_r is mainly controlled by the ratio of the differential rotation effect over the induced current (Ferreira & Pelletier 1995). No jet would be produced without differential rotation for it is the only cause of the vertical decrease of J_r. However, the counter current due to the differential rotation cannot be much bigger than the induced current in the disc, otherwise J_r would become strongly negative and lead to an unphysically positive toroidal field at the disc surface. Thus, steady state ejection is achieved only when these two effects are comparable, which translates into

$$\Lambda \sim \Lambda_c \equiv \frac{3 \chi_m}{\alpha_m^2 \mathcal{P}_m \varepsilon} \tag{2.66}$$

For $\Lambda > \Lambda_c$, matter is spun down at the disc surface, while for $\Lambda < \Lambda_c$ there is not enough energy to propell the large amount of mass trying to escape from the disc. Thus, equation (2.66) is a necessary condition for stationarity. Note that for χ_m and $\mathcal{P}_m$ of order unity, magnetized jets imply a dominant magnetic torque. For a turbulence parameter $\alpha_m \sim 1$, it translates into $\Lambda \sim \varepsilon^{-1}$.

[8]Namely, rotation, open field lines and some amount of diffusion allowing loading of matter.

From resistive discs to ideal MHD jets

As matter is expelled off the disc (by the plasma pressure gradient) with an angle $\theta_{u_p} \equiv \arctan(u_r/u_z)$, magnetic stresses make it gradually flow along a magnetic surface (with $\vec{u_p} \parallel \vec{B_p}$). Indeed, Ohm's law (2.31) can be written

$$\eta_m J_\phi = u_r B_z \left(\frac{\tan\theta_{B_p}}{\tan\theta_{u_p}} - 1 \right) \tag{2.67}$$

where $\theta_{B_p} \equiv \arctan(B_r/B_z)$. As long as $\theta_{u_p} < \theta_{B_p}$, the toroidal current remains positive. This maintains a negative vertical Lorentz force (that decreases u_z) and a positive radial Lorentz force (that, along with the centrifugal term, increases u_r), thus increasing θ_{u_p}. If $\theta_{u_p} > \theta_{B_p}$, the toroidal current becomes negative, lowering both components of the poloidal Lorentz force and, hence, decreasing θ_{u_p}. Therefore, in addition to the vertical decrease of the magnetic diffusivity (for its origin lies in a turbulence triggered inside the disc), there is a natural mechanism that allows a smooth transition between resistive to ideal MHD regimes.

2.4.2 Disc-jets interrelations

Dimensionless parameters

The accretion disc is defined by 11 variables, ie. the same 8 as in the ideal MHD jets plus the 3 transport coefficients. All these quantities can be calculated from their values at the disc equatorial plane. At a particular radius r_o they write

$$P_o = \rho_o \Omega_K^2 h^2$$

$$T_o = \frac{GMm_p}{k_B r_o}\varepsilon^2$$

$$u_{r,o} = -u_o = -m_s \varepsilon \Omega_K r_o \qquad \text{where} \quad m_s = 2q\mu\tfrac{1+\Lambda}{\delta\Lambda} = \alpha_v\varepsilon(1+\Lambda) = \alpha_m \mathcal{R}_m \varepsilon \mu^{1/2}$$

$$\left.\frac{du_z}{dz}\right|_{z=0} = \frac{u_o}{r}(\xi - 1)$$

$$\Omega_o = \delta\,\Omega_K \qquad \text{where} \quad \delta = \left(1 - \varepsilon^2\left[\frac{m_s^2}{2} + 2(2-\beta) + \mu\mathcal{R}_m\right]\right)^{1/2}$$

$$\rho_o = \frac{\dot{M}_{ao}}{4\pi\Omega_K r_o^3 m_s \varepsilon^2}$$

$$B_o = \left(\frac{\mu}{m_s}\right)^{1/2}\left(\frac{\mu_o \dot{M}_{ao}\Omega_K}{4\pi r_o}\right)^{1/2} \qquad \text{where} \quad \mu = \frac{B_o^2}{\mu_o P_o}$$

$$\left.\frac{dB_\phi}{dz}\right|_{z=0} = -\mu_o J_{r,o} = -q\frac{B_o}{h} \qquad \text{where} \quad q = \frac{\alpha_m \mathcal{P}_m \Lambda \varepsilon}{2\mu^{1/2}}\delta$$

$$J_{\phi,o} = \mathcal{R}_m \frac{B_o}{\mu_o r} \qquad \text{where} \quad \mathcal{R}_m = \mathcal{P}_m(1+\Lambda)$$

where $\alpha_v = \nu_v/\Omega_K h^2$, $\Omega_K = \sqrt{GM/r_o^3}$, $\dot{M}_{ao} = \dot{M}_a(r_o)$, $\beta = d\ln a/d\ln r_o$ provides the magnetic flux distribution and Λ is constrained by Eq. (2.66). Thus, there are 3 more parameters in addition to the previous 4 ones (ε, α_m, $\mathcal{P}_m$, χ_m) : the magnetic flux distribution β, the magnetic field strength μ and the ejection index ξ. The 3 regularity conditions arising at the 3 critical points met by the ejected plasma along each magnetic surface provide the value of 3 disc parameters (precisely, their values at the anchoring radius r_o). Inside our cold approximation, we therefore expect to fix the values of β, μ and ξ as functions[9] of the free parameters ε, α_m, $\mathcal{P}_m$ and χ_m. As a consequence, jet properties (ie. invariants as well as the asymptotic behaviour) arise as by-products of these parameters.

Using the set of ideal MHD equations, mass conservation gives a mass flux leaving the disc surface $\rho^+ u_z^+ \simeq \xi\varepsilon\rho_o u_o$ related by ξ to the accretion mass flux. Then, angular momentum conservation provides the following exact relations

$$\begin{aligned} \lambda &= 1 + \frac{\Lambda}{2\xi(1+\Lambda)}\left|\frac{B_\phi^+}{qB_o}\right| \simeq 1 + \frac{1}{2\xi} \\ \kappa &= \frac{q}{\lambda - 1}\left|\frac{B_\phi^+}{qB_o}\right| = \xi\frac{m_s}{\mu} \end{aligned} \tag{2.68}$$

Both magnetic lever arm λ and mass load κ are therefore determined by the ejection index ξ (which is directly related to the exact value of the toroidal field B_ϕ^+ at the disc surface[10]). One way to understand this point is to compute the ratio σ of the MHD Poynting flux to the kinetic energy flux. At the disc surfaces this ratio writes

$$\sigma_+ = \left|\frac{-\Omega_* r B_\phi \vec{B}_p}{\mu_o \frac{\rho u^2}{2}\vec{u}_p}\right|_+ = 2(\lambda - 1) = \frac{1}{\xi}\frac{\Lambda}{1+\Lambda}\left|\frac{B_\phi^+}{qB_o}\right| \simeq \frac{1}{\xi} \tag{2.69}$$

The ejection index appears to be also a measure of the power feeding the jets. For instance, relativistic jet models from keplerian accretion discs, requiring an initial (ie at the disc surface) "magnetization" σ_+ of order 10^6 can only be possible if the jets carry away all the disc angular momentum with a

[9] An important remark. The field strength cannot be too large ($\mu >> 1$), otherwise there will be no vertical equilibrium possible. On the other hand, if it is too small ($\mu << 1$), then the disc is prone to the magneto-rotational instability (Balbus & Hawley 1991). Therefore, we expect $\mu \sim 1$ in steady-state MAES. However, the allowed values of ξ strongly depend on the (subtle) vertical equilibrium and its interplay with the induction equation.

[10] The estimate $B_\phi^+ \simeq -qB_o$ is roughly acurate (by less than a factor 2) but the jet asymptotic structure highly depends on its precise value (Ferreira 1997).

tiny ejection efficiency of $\xi \sim 10^{-6}$! No such solution was ever found (see below). Nevertheless, unless ξ is of order unity, the magnetic field completely dominates matter at the disc surface (Eq. (2.66) forbids $1 >> \Lambda \sim \xi$).

Constraints on the ejection index of cold MAES

Can we provide any general constraint on the allowed range of ξ ? This is the trickiest question about MAES and here follows some analytical arguments in the simple case of cold jets from isothermal discs (Ferreira 1997).

The maximum value ξ_{max} is constrained by the jet capability to accelerate ejected matter, hence momentum conservation. Let's consider two extreme cases. Imagine there is such a tiny fraction of mass ejected that it takes almost no energy to accelerate it until the Alfvén point. But as some acceleration has been provided anyway, we can write $\sigma_A < \sigma_+$. On the other extreme, a huge amount of matter is expelled off the disc, which has hardly enough energy. In this most extreme case, no more energy is left after the Alfvén point and $m^2_{max} = 1$. Gathering these two conditions provides the constraint

$$\frac{1+2\xi}{1-4\xi} < \omega_A^2 < \frac{1}{2\xi} \tag{2.70}$$

which shows that cold jets (1) require $\omega_A > 1$ (fast rotators) and (2) display a maximum ejection efficiency of $\xi_{max} = \frac{\sqrt{13}-3}{4} \simeq 0.15$. Higher ejection indices are inconsistent with steady-state, trans-Alfvénic, cold jets.

The minimum value ξ_{min} of the ejection index is constrained by the disc vertical equilibrium. The diminishing of the ejection efficiency ξ is obtained by increasing the magnetic compression, especially through the radial component (via λ, increasing as ξ decreases). Now, to maintain the vertical balance while bending the field lines, but without increasing the plasma pressure, one must decrease the magnetic field amplitude (parameter μ). But then, there is a non-linear feedback on the toroidal field induction. Indeed, as μ decreases, the effect due to the differential rotation decreases also, leading to an increase of the toroidal field at the disc surface. This causes an increase of the toroidal magnetic pressure, hence an even greater magnetic squeezing of the disc. Below ξ_{min}, no vertical equilibrium is possible. Providing a quantitative analytical expression of how much matter can actually be ejected, ie. the value of ξ_{min}, is out of range. Indeed, in the resistive upper disc layers, **all dynamical terms are comparable** in Eq. (2.64). A careful treatment of the disc vertical balance is therefore badly needed. Thus, finding the correct parameter space of a MAES forbids the use of too strong approximations, such as $\rho u_z = constant$ (Wardle & Königl 1993), strict hydrostatic balance

(Li 1995) or any other prescription mimicking the induction equation (Li 1996).

Jet asymptotic structure

Can we relate the jet asymptotic structure to the disc parameters without solving the full set of MHD equations ? Naively, one would say that the larger λ the larger jet asymptotic radius, *if some cylindrical collimation is achieved*. Next section, we will see that this last issue is far from being obvious. Anyway, we can still safely say that if some current is still available after the Alfvén point, then magnetic acceleration will probably occur, along with an opening of the magnetic surfaces. In fact, the larger B_ϕ^+, the larger $B_{\phi,A}$. This, in turn, ensures that jets will provide a big acceleration and open up a lot. For a cold jet, the ratio I_A/I_+ of the remaining current I_A to the current provided at the disc surface I_+ is

$$\frac{I_A}{I_+} = \frac{r_A B_{\phi,A}}{r_o B_\phi^+} \simeq g_A \quad \text{where} \quad g_A^2 = 1 - \frac{3}{\lambda} - \frac{1}{\omega_A^2} + \frac{2}{\lambda^{3/2}(1+z_A^2/r_A^2)^{1/2}} \tag{2.71}$$

The expression of g_A is the Bernoulli equation evaluated at the Alfvén point and

$$\omega_A \simeq \kappa \lambda^{3/2} \frac{\sin(\phi_A - \theta_A)}{\sin \phi_A} \tag{2.72}$$

where ϕ_A is the local angle between the Alfvén surface (defined by $z = z_A(r_A)$) and the vertical axis, and θ_A the opening angle estimated at the Alfvén point. Both angles are determined by the resolution of the Grad-Shafranov equation, which takes into account radial boundary conditions. Note that this expression is only valid for a conical Alfvén surface, a geometry which arises naturally when jet parameters vary slowly across the jet. Since cold jets require fast magnetic rotators ($\omega_A > 1$), a necessary condition for trans-Alfvénic jets is $\kappa\lambda^{3/2} > 1$, which translates into $\lambda > (\Lambda \alpha_v \varepsilon)^{-2}$. Thus, jets launched from discs with a dominant viscous torque $\Lambda < 1$ require huge magnetic lever arms, namely $\lambda \gg \varepsilon^{-2}$. This is most probably forbidden by the disc vertical equilibrium that would not survive such a strong magnetic pinching. So, cold disc-driven jets are presumably carrying away a significant fraction of the disc angular momentum ($\Lambda > 1$).

Summary

From the preceeding general analysis, we can *a priori* expect two extreme **cold** configurations from quasi-keplerian discs :

Type I, where large toroidal currents J_ϕ at the disc midplane correspond to large magnetic Reynolds numbers $\mathcal{R}_m \sim \varepsilon^{-1} >> 1$ and a dominant magnetic torque $\Lambda \sim \varepsilon^{-1}$. This configuration would be achieved for isotropic turbulence, $\mathcal{P}_m \sim 1$ and $\chi_m \sim 1$.

Type II, where the dominant source of toroidal currents is at the disc surfaces, corresponding to straight field lines inside the disc ($\mathcal{R}_m \sim 1$) that become bent only at the surface. These surface currents come from the electromotive force ($J_\phi^+ \simeq -(u_r B_z/\eta_m)^+$), due to the presence of a large viscous torque ($\Lambda \sim 1$) allowing a non zero accretion velocity at the disc surface. Such a configuration would be achieved for an anisotropic turbulence, $\mathcal{P}_m > 1$ and $\chi_m \sim \varepsilon$.

At this stage, I hope the reader has achieved an understanding of the relevant physical mechanisms inside a keplerian accretion disc driving jets (question 1, Sect. 2.1.4). The disc physical conditions (question 2) are described by the MAES parameter space and thus, require the treatment of the complete set of MHD equations. As a "by-product", we will hopefully have the answer of the last question (jet properties).

2.5 Self-similar solutions of MAES

2.5.1 Self-similar Ansatz and numerical procedure

Solving the full set of MHD equations requires heavy 2D or 3D numerical simulations. However, looking for special solutions will allow us to transform the set of partial differential equations (PDE) into two sets of ordinary differential equations (ODE) with singularities. Gravity is expected to be the leading energy source and force in accretion discs. Thus, if MAES are settled on a wide range of disc radii, magnetic energy density probably follows the radial scaling imposed by the gravitational energy density. The gravitational potential writes in cylindrical coordinates

$$\Phi_G(r,z) = -\frac{GM}{r}\left(1+\frac{z^2}{r^2}\right)^{-1/2} \tag{2.73}$$

Since the disc is a system subjected to the dominant action of gravity, any physical quantity $A(r,z)$ will follow the same scaling, namely $A(r,z) = G_A(r) f_A(\frac{z}{r})$. Since gravity is a power law of the disc radius, we use the following self-similar Ansatz

$$A(r,z) = A_e \left(\frac{r}{r_e}\right)^{\alpha_A} f_A(x) \tag{2.74}$$

where $x = z/h(r) = z/\varepsilon r$ is our self-similar variable and r_e is the MAES outer radius. Because all quantities have power law dependencies, the resolution of the "radial" set of equations is trivial and provides algebraic relations between all exponents. The most general set of radial exponents allowing to take into account **all** terms in the dynamical equations (ie. no energy equation) is :

$$\begin{aligned} \beta &= \frac{3}{4} + \frac{\xi}{2} & \alpha_\rho &= \xi - \frac{3}{2} \\ \alpha_{B_r} = \alpha_{B_\phi} = \alpha_{B_z} &= \beta - 2 & \alpha_P &= \alpha_\rho - 1 \\ \alpha_{u_r} = \alpha_{u_\phi} = \alpha_{u_z} &= -\frac{1}{2} & \alpha_{\nu_m} = \alpha_{\nu'_m} &= \alpha_{\nu_v} = \frac{1}{2} \end{aligned}$$

As an illustration, the solutions obtained by Blandford & Payne used $\beta = 3/4$, ie $\xi = 0$. Note also that the disc scale height must verify $h(r) = \varepsilon r$. Such a behaviour stems only from dynamical considerations, ie. the vertical equilibrium between gravity and magnetic compressions and plasma pressure gradient. However, the energy equation provides another constraint that is usually incompatible with such a scaling (see eg. Ferreira & Pelletier 1993). We will come back to this issue later on.

All quantities $f_A(x)$ are obtained by solving a system of ODE which can be put into the form

$$\begin{pmatrix} \cdots & & \\ & \mathbf{M} & \\ & & \cdots \end{pmatrix} \cdot \begin{pmatrix} \frac{df_1}{dx} \\ \vdots \\ \frac{df_n}{dx} \end{pmatrix} = \begin{pmatrix} \cdots \\ \mathbf{P} \\ \cdots \end{pmatrix}$$

where $\mathbf{M}$ is a 8x8 matrix in resistive MHD regime, 6x6 in ideal MHD (see Ferreira & Pelletier 1995). A solution is therefore available whenever the matrix $\mathbf{M}$ is inversible, namely its determinant is non-zero. Starting in resistive MHD regime, $det\,\mathbf{M} = 0$ whenever

$$V^2(V^2 - C_s^2) = 0 \ , \tag{2.75}$$

where C_s is the sound speed and $V \equiv \vec{u}\cdot\vec{n}$ is the critical velocity. The vector

$$\vec{n} = \frac{\vec{e}_z - x\varepsilon\vec{e}_r}{(1 + x^2\varepsilon^2)} \tag{2.76}$$

provides the direction of propagation of waves that are consistent with our axisymmetric, self-similar description. Therefore, close to the disc, the critical velocity is $V \simeq u_z$, whereas far from the disc it becomes $V \simeq u_r$ (no

critical point in the azimuthal direction). Thus, inside the resistive disc, the anonalous magnetic resistivities produce such a dissipation (presence of high order derivatives) that the magnetic force does not act as a restoring force and the only relevant waves are sonic. Note also that the equatorial plane where $V = 0$ is also a critical point (of nodal type since all the solutions must pass through it). This introduces a small difficulty, since one must then begin the integration slightly above it. In the ideal MHD region, $det\,\mathbf{M} = 0$ whenever

$$(V^2 - V_{SM}^2)(V^2 - V_{FM}^2)(V^2 - V_{An}^2)^2 = 0 \tag{2.77}$$

namely, where the flow velocity V successively reaches the three phase speeds V_{SM}, V_{An} and V_{FM}, corresponding respectively to the slow magnetosonic wave, the Alfvén wave and the fast magnetosonic wave. The phase speeds of the two magnetosonic modes have the usual expression, namely $V_{SM,FM}^2 = \frac{1}{2}\left(C_s^2 + V_{At}^2 \mp \sqrt{(C_s^2 + V_{At}^2)^2 - 4C_s^2 V_{An}^2}\right)$ where V_{At} is the total Alfvén speed and $V_{An} = \vec{V}_{Ap}\cdot\vec{n}$. Note that the condition $V = V_{An}$ is equivalent to $u_p = V_{Ap}$, which shows that this is the usual Alfvénic critical point encountered in jet theories. It is also noteworthy to remark that the multiplicity of this root implies that at the Alfvénic point, both first and second order derivatives of the physical quantities are imposed by the regularity condition.

How do we proceed ? Starting slightly above the disc midplane where all quantities are known, we propagate the resistive set of equations using a Runge-Kutta (better a Stoer-Burlisch) solver. We do this for fixed values of the four free parameters $(\varepsilon, \alpha_m, \chi_m, \mathcal{P}_m)$ and some guesses for μ and ξ. As x increases, the flow reaches an ideal MHD regime and we shift to the corresponding set of equations. Care must be taken in order to not introduce jumps in the solution while doing this. If, for the chosen ejection efficiency ξ, the value μ of the magnetic field is too large, the overwhelming magnetic squeezing leads to a decrease of u_z. If, on the contrary, μ is too small, the plasma pressure gradient becomes far too efficient and leads to infinite vertical acceleration. Using these two criteria and fine-tunning μ, we can approach the SM point so close that a simple linear extrapolation on all quantities allow us to safely cross the singularity. This leapfrog must not introduce any discontinuity (to some tolerance) on all jet invariants. By doing so, we obtain a trans-SM solution. This is done for a chosen value of ξ that may not be the critical ξ_c allowing a trans-A solution. If $\xi < \xi_c$, the magnetic tension wins over the outwardly directed tension produced by the ejected, rotating plasma. As a result, the magnetic surface closes which leads to a decceleration and the Alfvén point is not reached. On the other hand, $\xi > \xi_c$ produces an over-opening of the magnetic surface leading to the unphysical situation where B_ϕ goes to zero. Again, once close to the Alfvén point (typically, $m = 1$ by

1%), we do a leapfrog. Thus, fine-tunning ξ and, for each guess, finding the critical value of μ, allow us to obtain trans-SM and super-Alfvénic solutions. No trans-FM self-similar "cold" solution *connected to the disc* can be found (see however Vlahakis et al (2000), for a generalization of the Blandford & Payne jet model). The proof of this is given in Ferreira & Casse (2004).

2.5.2 "Cold" configurations

A cold configuration is defined by a negligible enthalpy at the disc surface (at each magnetic surface). Since discs are quasi-keplerian, cold jets are obtained with an isothermal (Wardle & Königl 1993, Ferreira & Pelletier 1995, Li 1995, 1996, Ferreira 1997) or adiabatic (Casse & Ferreira 2000a) *vertical* profile $f_T(x)$ of the temperature.

General behaviour

The general behaviour is exactly that expected in the disc. Both magnetic and (if non negligible) turbulent viscous torques extract energy and angular momentum from disc plasma. The accretion velocity depends on the amount of magnetic diffusivity. As plasma is being accreted from the outer disc regions, it is slightly converging towards the disc midplane (because of both tidal and magnetic compressions). Matter located (locally) at the disc surface feels a strong outwardly directed magnetic tension and a positive azimuthal torque, both arising from current consommation ($\nabla_\parallel I > 0$) : accretion is stopped and reversed. More or less simultaneously, a positive vertical velocity is provided by the plasma pressure gradient.

Ejected matter leaves the disc with a vertical velocity initially much smaller than the local sound speed, $u_z^+ \simeq m_s \xi C_s$. It gets however very quickly accelerated as it leaves the resistive MHD zone. The SM point lies typically between 1 and 2 scale heights, usually at the very beginning of the ideal MHD zone. Until the Alfvén point, plasma is almost co-rotating with the magnetic field lines, behaving like a rigid funnel. The Alfvén point is far away above the disc, at an altitude $z_A \sim r_A = \lambda^{1/2} r_o \gg h(r_o)$. After its crossing, there is a sudden opening of the magnetic surfaces. This is due to the centrifugal force which is now enhanced by the tension provided by the super-Alfvénic flow ($m^2 > 1$, see Eq. 2.46). This opening of the magnetic surfaces is controlled by the quantity ω_A : the larger ω_A, the larger maximum jet radius. Or, the less current used in the sub-A region and the more remains in the super-A region.

As the magnetic surface opens up, plasma drags along the field lines which produces a large toroidal field. This is the consequence of ideal MHD since

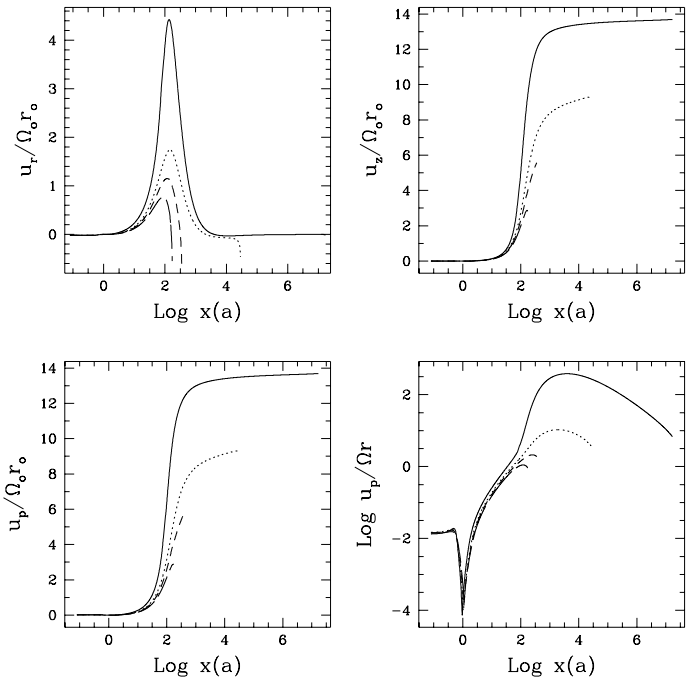

FIG. 2.4 – Components of the jet poloidal velocity $\vec{u}_p$ and ratio of the poloidal to the toroidal velocities, measured along a magnetic surface and different ejection indices : $\xi = 0.005$ (solid line), $\xi = 0.01$ (dotted line), $\xi = 0.02$ (short-dashed line) and $\xi = 0.05$ (long-dashed line). Note that the poloidal velocity is almost zero at the disc surface ($x \sim 1$).

matter is rotating **slower** than the field lines ($\Omega < \Omega_*$). As the toroidal field increases, the "hoop stress" becomes more and more important until it overcomes the centrifugal force. This is unavoidable if the jet can open up freely in space (negligible outer pressure) and if its inner transverse equilibrium allow it : the centrifugal effect decreases faster with radius than the hoop-stress. As a result, the cold jet asymptotic transverse equilibrium is simply given by

$$-\nabla_\perp \left(P_{ext} + \frac{B^2}{2\mu_o} \right) = \frac{B_\phi^2}{\mu_o r} \nabla_\perp r \tag{2.78}$$

where P_{ext} must be understood here as the pressure of the material located on the axis or outside the jet. A strict cylindrical collimation requires therefore a perfect (and fragile) matching between the hoop-stress and the total pressure gradient. In our self-similar solutions, $P_{ext} = 0$ and the inner magnetic field

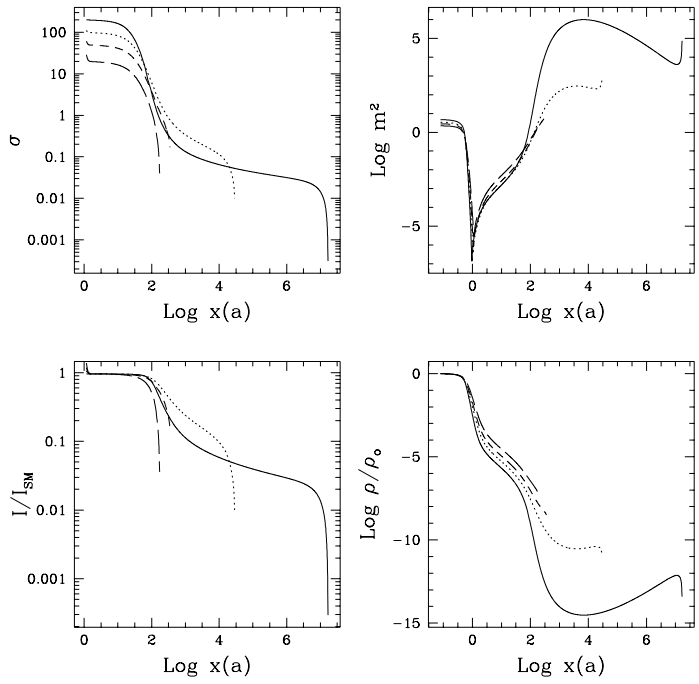

FIG. 2.5 – Ratio σ of the MHD Poynting flux to the kinetic energy flux, logarithm of the Alfvénic Mach number m^2, total poloidal current I embraced by the magnetic surface (normalized to its value at the disc surface) and plasma density logarithm along a magnetic surface. The different curves are for the same parameters as in Fig. 2.4.

gradient is not enough to balance the hoop-stress. As a consequence, all solutions recollimate (refocus) towards the jet axis.

This seems to be a (quite) general result of MHD jets that can freely expand in space. For example, all Blandford & Payne disc wind solutions and X-wind solutions obtained by Shu et al. (1995) also recollimate[11]. However, Contopoulos & Lovelace (1994) as well as Ostriker (1997) obtained solutions within the same self-similar ansatz that did not recollimate : recollimation is therefore not a feature of self-similarity alone. On the other hand, Pelletier & Pudritz (1992) found recollimating solutions that are not self-similar. In

[11]Shu et al. imposed however a cylindrical asymptotic collimation by assuming an equilibrium between the jet hoop-stress and an inner magnetic pressure, provided by a poloidal field located on the axis.

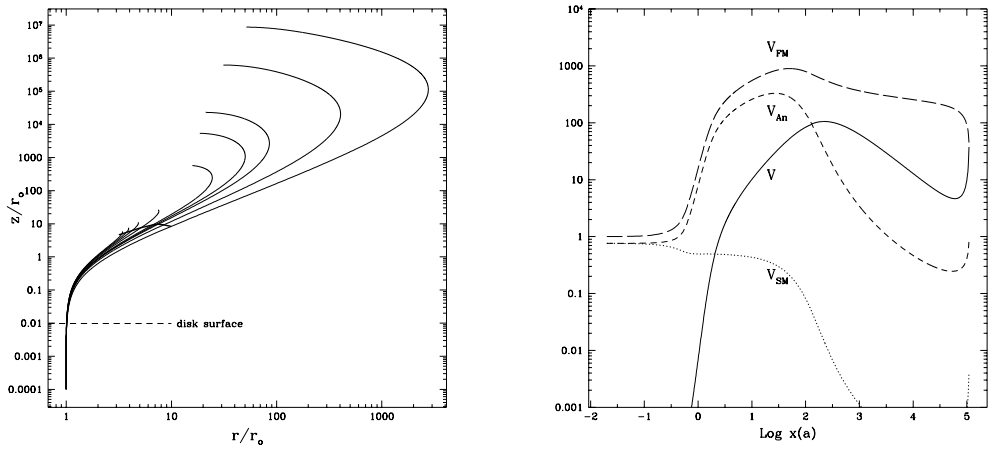

FIG. 2.6 – **Left** : Poloidal magnetic surfaces for $\varepsilon = 0.01$ and $\alpha_m = 1$ and different ejection indices (hence ω_A) : $\xi = 0.05$, 0.04, 0.03, 0.02, 0.012, 0.01, 0.009, 0.007 and 0.005 (the maximum radius increases with decreasing ξ). The thick line connects the Alfvén points of each surface, anchored at a radius r_o. **Right** : Critical speed $V = \vec{u} \cdot \vec{n}$ and phase speeds V_{SM}, V_{An}, V_{FM} (corresponding respectively to the SM, Alfvén and FM waves) along a magnetic surface. All speeds are normalized to the disc sound speed $\Omega_K h_o$. The SM point lies just above the disc surface at $z_{SM} \sim h$, while the Alfvén point is at $z_A \sim r_A$ (here $\sim 10 r_o$). The solution shown here does not cross the last (FM) critical point (although $u_p > V_{FM}$).

fact, it is possible to show that if the conditions

$$\frac{d\ln\lambda}{d\ln r_o} > 1 \qquad \text{and} \qquad \frac{d\ln(\rho_A/\rho_o)}{d\ln r_o} < \frac{d\ln\rho_o}{d\ln r_o} = \alpha_\rho \tag{2.79}$$

are satisfied in a cold, disc-driven jet, then recollimation would have been impossible (Ferreira 1997). Evidently, such conditions are violated in self-similar solutions : λ and ρ_A/ρ_o remain constant throughout the jet. However, this analytical analysis shows that non self-similar jets produced from a large range of disc radii and displaying no strong gradients of these quantities may be prone to recollimation (as in Pelletier & Pudritz).

What happens to our solutions after they recollimate ? When the jet transverse equilibrium enforces recollimation, almost all available angular momentum has already been transfered to matter and $\Omega \simeq \Omega_* r_A^2/r^2$. This implies that the current also goes to zero $I \to 0$ (and not a constant) and so does the toroidal field. The recollimating matter drags the field lines

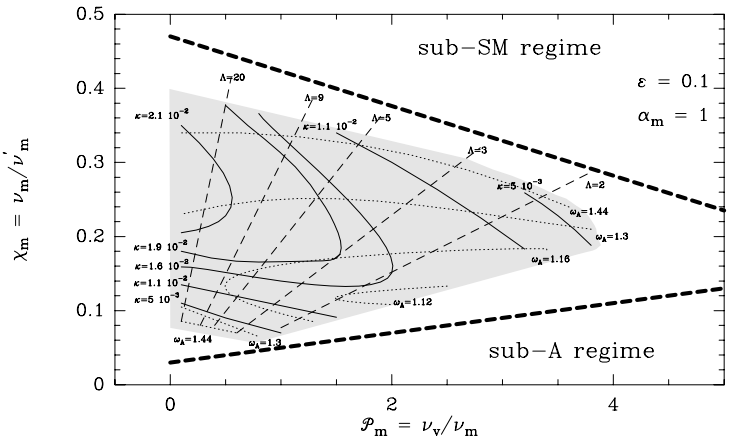

FIG. 2.7 – Parameter space of cold, adiabatic MAES for $\alpha_m = 1$, $\varepsilon = 0.1$. The shaded areas correspond to the location where numerical solutions could be found. The thick dashed lines show theoretical limits, corresponding to no super-SM flows (upper line) and no super-A flows (lower line).

along with it, severely reducing the pitch of the magnetic helix. Before B_ϕ reaches zero, our self-similar solution meets the last critical point, namely $V \sim u_r = V_{FM} \sim V_{At}$ (note that $u_p > V_{FM}$ already before recollimation). Vlahakis et al. (2000) obtained super-FM solutions by playing with the location of the Alfvén surface and the jet polytropic index. But these solutions are terminated in the same way as those displayed here. Such a behaviour remains unexplained and may be due to the self-similar form of the solutions. Anyway, such super-FM solutions could safely produce an oblique shock[12] leading to a time-dependent readjustment of the whole structure. This will not alter the underlying steady-state solution, for no signal can propagate upstream. Although Vlahakis et al. solutions are not connected with the disc, their work gives an indication that introducing another degree of freedom (the polytropic index value) might indeed provide trans-FM solutions. But in any case, at this stage, a shock seems the unavoidable fate of this mathematical class of solutions.

Parameter space of cold, adiabatic MAES

The parameter space of cold MAES is obtained by varying the set of free disc parameters $(\varepsilon, \alpha_m, \mathcal{P}_m, \chi_m)$. We choose to fix the values of both ε and α_m and represent the parameter space with the remaining parameters

[12] As suggested by Gomez de Castro & Pudritz (1993) and maybe seen in numerical simulations of Ouyed & Pudritz (1997).

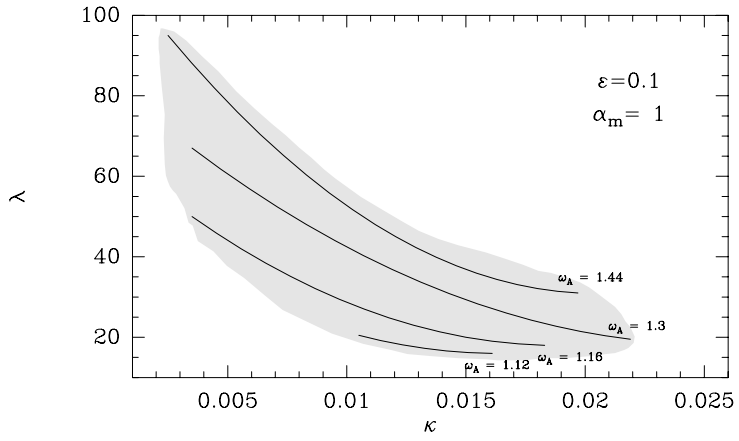

FIG. 2.8 – Jet $\kappa - \lambda$ parameter space of cold, adiabatic MAES for $\alpha_m = 1$, $\varepsilon = 0.1$. The shaded areas correspond to the location where numerical solutions could be found. This parameter space is much narrower than those found by Blandford & Payne (1982), Wardle & Königl (1993) and Li (1995).

(Fig. 2.7 and 2.8). Numerical solutions are only found inside the shaded areas, where we also plot levels of two jet parameters ω_A and κ. This region is embedded inside a larger region (thick dashed lines), obtained by two analytical constraints. The first one arises from the requirement that jets become super-SM and is thus related to the disc vertical equilibrium. The second emerges from the requirement that jets must become super-Alfvénic, namely $\omega_A > 1$, providing the lower limits in the same plots. These two analytical constraints strongly depend on both α_m and ε. Cold, adiabatic MAES have the following properties :

• The parameter space is very narrow, with typical values $\xi \sim 10^{-2}$ and $\mu \sim 1$, with the following approximate scaling

$$\xi \sim 0.1\,\mu^3 \tag{2.80}$$

Although its validity holds only in a quite narrow interval, it shows that *the stronger the field the more mass is ejected*. No solution has been found outside the range $0.001 < \varepsilon < 0.3$ and $0.3 \leq \alpha_m < 3$. The corresponding jet parameters lie in the range $10 < \lambda < 100$ and $0.001 < \kappa < 0.03$.

• The parameter space shrinks considerably with α_m, because of the extreme sensibility of B_ϕ^+ to it (Casse & Ferreira 2000a). Note however that $\alpha_v = \alpha_m \mu^{1/2} \mathcal{P}_m$ is usually smaller than α_m.

• No solution has been found with a dominant viscous torque ($\Lambda \ll 1$) : the reason lies in the imposed geometry of the Alfvén surface (conical). On

the other hand, high-ω_A solutions (those with large jet radius) exist only for magnetically-dominated discs ($\Lambda \gg 1$).

• The required turbulence anisotropy increases with both Λ and α_m, following the scaling $\chi_m \sim \Lambda\varepsilon\alpha_v\alpha_m$ provided by Eq. (2.66).

2.5.3 "Warm" configurations

Entropy generation inside the disc

As seen in Sect. 2.2.3, the disc energy equation (2.34) is such a mess that all works on accretion discs used simplified assumptions. In fact using an isothermal or adiabatic prescription for the temperature vertical profile may be an over simplification, that may have led to such a small parameter space. One way to tackle the energy equation is to solve

$$\rho T \frac{dS}{dt} = \rho T \vec{u}_p \cdot \nabla S = Q \tag{2.81}$$

where the entropy source $Q = \Gamma - \Lambda$ is prescribed and describes the *local net* effect of all possible heating Γ and cooling Λ terms. The sources of heating are :

$\hookrightarrow$ $\Gamma_{eff} = \eta_m J_\phi^2 + \eta'_m J_p^2 + \eta_v |r\nabla\Omega|^2$ the effective Joule and viscous dissipations ;

$\hookrightarrow$ Γ_{turb} due to turbulent energy deposition, not described by anomalous coefficients ;

$\hookrightarrow$ Γ_{ext} some external source of energy (like protostellar UV or X-rays, or cosmic rays).

On the other hand, the cooling sources are

$\hookrightarrow$ $\Lambda_{rad} = \nabla \cdot \vec{S}_{rad}$ radiative losses in optically thick or thin media ;

$\hookrightarrow$ Λ_{turb} turbulent transport that may be described by kinetic theory or due to large scale motions like convection (in Eq. (2.34) $\nabla \cdot \vec{q}_{turb} = \Lambda_{turb} - \Gamma_{turb}$).

In our simplified approach, we prescribe both the shape and amplitude of Q, but consistently with energy conservation. We make therefore two assumptions : (1) there is no net input of turbulent energy in the volume $\mathcal{V}$ occupied by the MAES, namely $P_{turb} = \int_{\mathcal{V}} (\Gamma - \Lambda)_{turb} \, d^3\mathcal{V} = 0$ and (2) the power deposited by any external medium is negligible, ie. $P_{ext} = \int_{\mathcal{V}} \Gamma_{ext} d^3\mathcal{V} = 0$. With these assumptions, the only remaining source of energy is accretion of the laminar flow : turbulence can only redistribute energy from one place to another one.

Accretion is possible because of the torque due to the mean magnetic field (jet) and the turbulent ("viscous") torque. Accretion energy released by

the first torque is converted into a MHD Poynting flux leaving the disc (and feeding the jets) and heat through local Joule dissipation. Accretion energy released by the "viscous" torque is conventionally thought as being converted into heat through dissipation. But note that if such a torque arises from field lines connecting two disc radii, one would then expect also an outward flux of energy, which would be dissipated above the disc surface (Galeev et al. 1979, Heyvaerts & Priest 1989, Miller & Stone 2000, Machida et al. 2000). Anyway, these two heating sources (Γ_{eff}) build up a local gas thermal energy reservoir which decreases because of the local cooling terms. Thus, the total power related to dissipation inside the disc (ie. not directly put into the jets) is $P_{diss} = \int_{\mathcal{V}} \Gamma_{eff} d^3\mathcal{V}$. In a conventional picture of accretion discs, such a power is finally radiated away, either at the disc surfaces only, or also in some chromosphere. Here, we assume that a fraction f of this power is in fact not lost by the plasma but provides an extra source of entropy Q, namely

$$f = \frac{\int_{\mathcal{V}} Q d^3\mathcal{V}}{\int_{\mathcal{V}} \Gamma_{eff} d^3\mathcal{V}} \tag{2.82}$$

This expression is consistent with global energy conservation, the parameter f being free and varying from 0 ("cold" MAES) to 1 ("warm" or magneto-thermally driven jets). A value of f larger than unity would require an extra source of energy. We need now to specify the vertical (self-similar) profile of Q. Obviously, this introduces so many degrees of freedom that we do not dare anymore to look for the parameter space. Instead, we will look for extreme configurations and try to derive quantitative results.

Dynamical effects

The steady-state energy equation (2.81) can be explicitely written

$$Q = \rho T \frac{dS}{dt} = \rho \frac{dH}{dt} - \frac{dP}{dt} = \frac{\gamma}{\gamma - 1} \frac{k_B}{m_p} \rho \vec{u}_p \cdot \nabla T - \vec{u}_p \cdot \nabla P \ . \tag{2.83}$$

where γ is the adiabatic index. We then see that the main influence of a non-zero Q is on the temperature and pressure vertical gradients (thin disc), thus at the disc surface. But this is precisely the place where such gradients are required for ejection (Sect. 2.4.1) ! Therefore, allowing some energy deposition at the disc surface has two major effects :

– (1) The initial jet temperature (T^+) is increased and may thereby provide a non-negligible initial enthalpy H ("warm" jets). Indeed, the Bernoulli integral becomes

$$E(a) = \frac{u^2}{2} \ + \ H \ + \ \Phi_G \ - \ \Omega_* \frac{r B_\phi}{\eta} \ - \ \int_{s^+}^{s} \frac{Q(s',a)}{\rho(s',a) u_p(s',a)} ds' \tag{2.84}$$

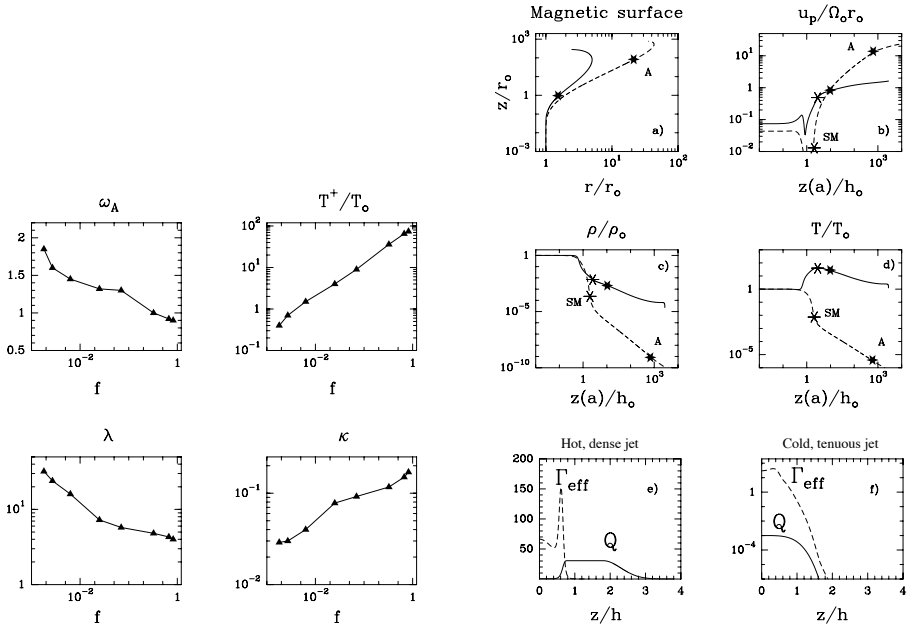

FIG. 2.9 – **Left** : Variation of jet parameters with f. As f increases, jets get hotter, denser and with a smaller magnetic lever arm λ. After some threshold, depending on the other MAES (turbulence) parameters, thermal effects become so important that super-A jets can be obtained with slow-rotators ($\omega_A < 1$). **Right** : Two new extreme MAES with an additional heating Q. If Q is very large at the disc surface ($f \sim 1$), hot and dense jets are produced (solid curves) whereas cold and very tenuous jets (dashed curves) are obtained if Q is almost inexistent ($f = 5\ 10^{-5}$). Lower pannels show the effective turbulent heating Γ_{eff} and the prescribed entropy source Q at a radius r_o, normalized to the same quantity.

where s is a curvilinear coordinate along the magnetic surface and s^+ represents the disc surface. If Q remains positive above s^+, it offers an additional energy reservoir for plasma. Moreover, the total energy feeding a magnetic surface,

$$E(a) = \frac{\Omega_o^2 r_o^2}{2}\left(2\lambda - 3 + \frac{2\gamma}{\gamma-1}\frac{T^+}{T_o}\varepsilon^2\right) \ . \tag{2.85}$$

is affected by the heating that already occurred in the underlying layers. Such an heating may provide a ratio T^+/T_o larger than unity, possibly allowing to relax the constraint on minimum field lines inclination.

– (2) If Q is relevant in the upper resistive layers, then it will increase also the plasma pressure gradient. This will enhance the ejected mass

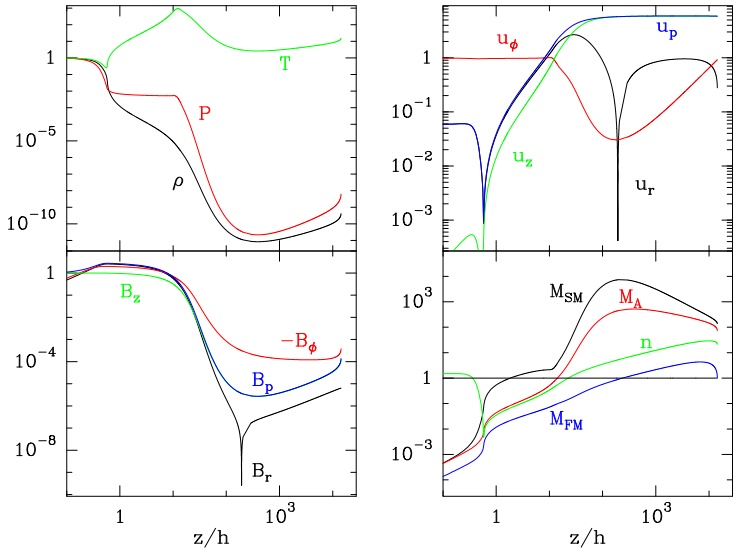

FIG. 2.10 – Typical super-FM disc wind with $\xi = 0.03, \epsilon = 0.03$ ($h = \epsilon r$). Density, pressure and temperature are normalized to their value at the disc midplane, the magnetic field components to $B_z(z = 0)$ and the velocities to the keplerian speed at the anchoring radius r_o. All magnetic field components remain comparable from the disk surface to the Alfvén point. Note that the density profile inside the disc, where both u_r and u_z are negative, is very different from a gaussian. Recollimation takes place at $z \simeq 3\ 10^3 r_o$. The lower right panel shows the various critical Mach numbers (e.g. $M_{SM} = V/V_{SM}$) appearing in the self-similar equations. The usual fast Mach number, $n = u_p/u_{FM}$, becomes greater than unity much sooner than the critical one $M_{FM} = V/V_{FM}$ (Ferreira & Casse 2004).

flux (and lower the magnetic lever arm) and might therefore have tremendous consequences on jet dynamics.

We used only one type of vertical profile $f_Q(s)$, changing the value of the parameter f. The chosen profile provides $Q \simeq 0$ inside the disc ($x < 0.5$), an increase until a maximum value (fixed by f) around $x \leq 1$, then a decrease to zero (adiabatic behaviour) after roughly one scale height (see Casse & Ferreira 2000b). As f increases (all other MAES parameters being held constant), one goes from cold ($T^+ < T_o$), tenuous ($\kappa < 0.02$) jets from fast rotators ($\omega_A > 1$) to hot ($T^+ \gg T_o$), dense ($\kappa > 0.1$) jets from slow rotators ($\omega_A < 1$). Namely, the presence of some chromospheric heating allows a smooth transition from "cold" (purely magnetically-driven) to "warm"

(magneto-thermaly driven) jets.

Prescribing a non zero function Q in the sub-Alfvénic jet region only, with subsequent adiabatic or polytropic dynamics, leads to very interesting results. This mimics the effect of some "coronal" heating as in the solar wind or, alternatively, the pressure due to an inner flow (e.g. stellar or magnetospheric wind) ramming into the disc wind. Because of this additional pressure, the field lines are forced to open much more than they would normally, leading to a different jet dynamical behaviour. In particular, self-similar jets can now smoothly cross the last modified FM critical point (Vlahakis et al 2000, Ferreira & Casse 2004). See Fig. 2.10 for an example. It has been shown that only such special circumstances could allow these mathematical solutions to cross the three MHD critical points.

Another class of "cold" solutions can also be designed. Indeed, if local cooling is not sufficient inside the disc ($Q > 0$ for $x < 1$), the plasma pressure increases which provides the disc a stronger support against both tidal and magnetic compression. As a result, the magnetic field lines can be more bent than in the previous adiabatic or isothermal solutions. Such a large curvature hinders mass to be ejected (κ may be as small as 10^{-4} and $\lambda \sim 400$) but a vertical equilibrium can nevertheless be reached[13]. Thus, entropy generation inside the disc removes the limits found on the "cold" parameter space described earlier.

Global energy conservation

We suppose that a MAES is settled around a central object of mass M, between an inner radius r_i and some outer radius r_e. At this outer radius, the structure is fed with an accretion rate $\dot{M}_{ae} = \dot{M}_a(r_e)$. Mass conservation then writes $\dot{M}_{ae} - 2\dot{M}_j = \dot{M}_{ai}$ and the fraction of ejected mass is

$$\frac{2\dot{M}_j}{\dot{M}_{ae}} = 1 - \left(\frac{r_i}{r_e}\right)^{\xi} \simeq \xi \ln \frac{r_e}{r_i} \tag{2.86}$$

the last expression being valid only for a very small ejection efficiency $\xi \ll 1$. The local energy conservation equation is

$$\nabla\cdot\left[\rho\vec{u}_p\left(\frac{u^2}{2} + \Phi_G + H\right) + \vec{S}_{MHD} - \vec{u}\cdot\mathsf{T}\right] = \rho T\vec{u}_p\cdot\nabla S - \Gamma_{eff} \tag{2.87}$$

whereas the second law of thermodynamics (2.81) provides

$$Q = \rho T\vec{u}_p\cdot\nabla S = \Gamma_{eff} + (\Gamma_{turb} - \Lambda_{turb}) + \Gamma_{ext} - \nabla\cdot\vec{S}_{rad} \tag{2.88}$$

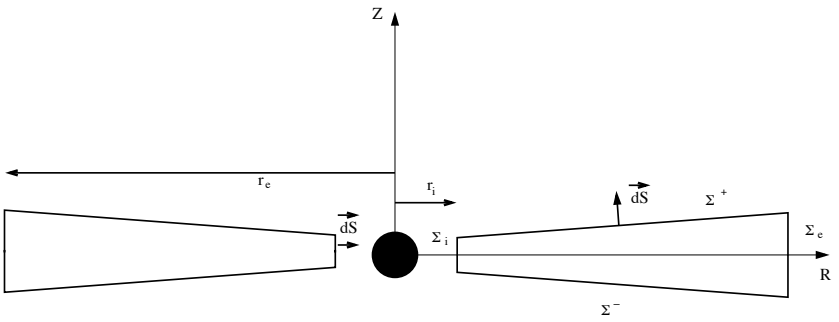

FIG. 2.11 – Sketch of the volume used for the calculation of the global energy conservation.

To get the global energy conservation, we integrate this equation on the volume $\mathcal{V}$ occupied by the disc. We thus define Σ^+ and Σ^- as the disc surfaces[14] and Σ_i (Σ_e) the lateral surfaces at $r = r_i$ ($r = r_e$, see Fig. (2.11)). After integration, we get

$$P_{acc} + P_{ext} + P_{turb} = 2P_{jet} + 2P_{rad} \tag{2.89}$$

where the accretion power P_{acc}, ie. the power released by the accretion flow, is the difference between what comes in at r_e and goes out at r_i. As said previously, we assumed $P_{ext} = P_{turb} = 0$ (neither an external source of energy, nor a significant input of turbulent energy). Thus, all available power P_{acc} is shared between radiative losses at the disc surfaces $P_{rad} = \int_{\Sigma^\pm} \vec{S}_{rad} \cdot d\vec{\Sigma}$ and jet power $P_{jet} = \int_{\Sigma^\pm} \rho \vec{u_p} E(a) \cdot d\vec{\Sigma}$. It is usefull to introduce the *fiducial* quantity

$$P_{lib} \equiv \eta_{lib} \frac{GM\dot{M}_{ae}}{2r_i} \simeq 2.5\,10^{32} \left(\frac{M}{M_\odot}\right) \left(\frac{\dot{M}_{ae}}{10^{-7} M_\odot/yr}\right) \left(\frac{r_i}{0.1 \text{ AU}}\right)^{-1} \text{ erg s}^{-1} \tag{2.90}$$

where η_{lib} is a term roughly equal to unity. Within our self-similar framework,

[13]Note that mildly relativistic speeds are expected if such a MAES is settled around a compact object.

[14]The disc surface $z = z^+ = x^+ h(r)$ is precisely defined as the locus where $u_r(r, z^+) = 0$.

energy conservation of a thin (or slim) disc writes

$$\frac{P_{acc}}{P_{lib}} = (1-\xi)\left(1+\frac{1}{2}\frac{\varepsilon\Lambda}{1+\Lambda}\right) \quad (2.91)$$

$$\frac{2P_{jet}}{P_{lib}} = \frac{\Lambda}{1+\Lambda}\left|\frac{B_\phi^+}{qB_o}\right| + \frac{2\gamma}{\gamma-1}\frac{T^+}{T_o}\xi\varepsilon^2 - \xi \quad (2.92)$$

$$\frac{2P_{rad}}{P_{lib}} = (1-f)\frac{P_{diss}}{P_{lib}} = \frac{P_{acc}-2P_{jet}}{P_{lib}} \quad (2.93)$$

See Casse & Ferreira (2000b) for the derivation of these expressions. Three important remarks. First, the absolute limit for the ejection efficiency is $\xi = 1$; Second, the real energy release is P_{acc}, comparable to P_{lib} only for low ejection indices. Finally, the MHD Poynting flux feeding the jets depends directly on the amount of toroidal field at the disc surface. Thus, magnetically-dominated discs ($\Lambda \gg 1$) may still produce some disc luminosity, provided $|B_\phi^+| < qB_o$ (and $f < 1$). For $f \sim 0$ we found solutions with a ratio P_{jet}/P_{lib} varying between 0.5 and 0.99.

Preliminary conclusions

From this study, we are forced to conclude that thermal effects have an outrageous quantitative importance on jet launching. In a way, this is fortunate since we can now recover and understand the parameter space obtained with numerical MHD simulations. Although "cold", the simulated jets have enormous mass loads and correspondingly small magnetic lever arms (eg. $\kappa \sim 0.6$, $\lambda \sim 3.5$, Ouyed & Pudritz 1999). This could be achieved from an accretion disc where a significant entropy generation took place at the disc surface ($f > 0.1$), followed right afterwards by a strong cooling ($Q < 0$ for $x > 1$). In this way, very dense but cold (well, after some time) jets can indeed be produced. Remember however that the bottom of the computational box (the "platform") is not the real disc surface.

A major drawback of such a conclusion is that any quantitative prediction (eg. the value of ξ) requires to treat the energy equation. We must therefore inject our knowledge on MHD turbulence and its (possibly non local) energy transport properties! Besides, illumination effects by the central protostar may also be important (since it heats up the disc surface).

2.5.4 Observational predictions

Accretion discs

Whether or not the disc remains geometrically thin depends on its internal temperature, hence on the energy equation. Although the energy transport processes are unknown, an opaque disc must radiate at its surfaces all deposited energy. Assuming a non flaring disc, the power balance at an annulus dr is

$$2 \times 2\pi r dr\ \sigma T_{eff}^4 = \dot{M}_a\ d\left(-\chi \frac{GM}{2r}\right) = \chi \frac{GM\dot{M}_a}{2r^2} dr \qquad (2.94)$$

where $\chi = 1$ for a standard accretion disc but only $\chi = 1/(1+\Lambda) \sim \varepsilon = h/r$ in a magnetized accretion disc driving jets. If the vertical transport of energy within the disc is by radiation diffusion, then the effective and central temperatures can be related through $T_{eff} \sim T_o \tau^{-1/4}$ where $\tau = \kappa \rho_o h$ is the disc optical depth. The disc midplane temperature and density are given by

$$\begin{aligned} T_o &= 5.8\ 10^4\ \varepsilon^2\ \left(\frac{M}{M_\odot}\right)\left(\frac{r}{1\ \mathrm{AU}}\right)^{-1}\ \mathrm{K} \\ n_o &= 4.7\ 10^6\ m_s^{-1}\varepsilon^{-2}\ \left(\frac{\dot{M}_a}{10^{-7}M_\odot/yr}\right)\left(\frac{M}{M_\odot}\right)^{-1/2}\left(\frac{r}{1\ \mathrm{AU}}\right)^{-3/2}\ \mathrm{cm}^{-3} \end{aligned}$$

It can be seen right away that, for the same accretion rate, a disc producing self-confined jets with $m_s \sim 1$ is much less dense than a standard accretion disc where $m_s = \alpha_v \varepsilon \ll 1$.

In order to obtain easy-to-handle expressions, I use the analytical fits of opacity tables given by Bell & Lin (1994). In the regime where metal grains dominate, one gets $\kappa = 0.1\ T^{1/2}\ \mathrm{cm^2 g^{-1}}$. This allows us to close our little system of equations and obtain the expression of ε as a function of the stellar mass M, disc accretion rate $\dot{M}_a$ and disc radius r. The following values are

henceforth derived :

$$
\begin{aligned}
\varepsilon &= 2\ 10^{-2} \left(\frac{\dot{M}_a}{10^{-6} M_\odot/yr}\right)^{2/7} \left(\frac{M}{M_\odot}\right)^{-3/7} \\
n_o &= 5.3\ 10^{10} \left(\frac{\dot{M}_a}{10^{-6} M_\odot/yr}\right)^{3/7} \left(\frac{M}{M_\odot}\right)^{5/14} \left(\frac{r}{1\ \mathrm{AU}}\right)^{-3/2}\ \mathrm{cm}^{-3} \\
\Sigma_o &= 2\rho_o h = 0.1 \left(\frac{\dot{M}_a}{10^{-6} M_\odot/yr}\right)^{5/7} \left(\frac{M}{M_\odot}\right)^{-1/14} \left(\frac{r}{1\ \mathrm{AU}}\right)^{-1/2}\ \mathrm{cm}^{-2} \\
T_o &= 92 \left(\frac{\dot{M}_a}{10^{-6} M_\odot/yr}\right)^{4/7} \left(\frac{M}{M_\odot}\right)^{1/7} \left(\frac{r}{1\ \mathrm{AU}}\right)^{-1}\ \mathrm{K} \\
T_{eff} &= 47.6 \left(\frac{\dot{M}_a}{10^{-6} M_\odot/yr}\right)^{9/28} \left(\frac{M}{M_\odot}\right)^{1/7} \left(\frac{r}{1\ \mathrm{AU}}\right)^{-3/4}\ \mathrm{K} \\
B_z &\simeq 0.6 \left(\frac{\dot{M}_a}{10^{-6} M_\odot/yr}\right)^{1/2} \left(\frac{M}{M_\odot}\right)^{1/4} \left(\frac{r}{1\ \mathrm{AU}}\right)^{-5/4}\ \mathrm{G} \\
\tau &= 5.1 \left(\frac{\dot{M}_a}{10^{-6} M_\odot/yr}\right) \left(\frac{r}{1\ \mathrm{AU}}\right)^{-1}
\end{aligned}
$$

for an accretion rate typical of DG Tau, a T Tauri star and jet source which has been extensively studied. For such an accretion rate, the inner parts of the circumstellar accretion disc where this opacity regime dominates are indeed optically thick, providing us with a consistent accretion-ejection picture. Note that for this particular opacity regime the self-similar regime $h(r) \propto r$ is apparently[15] strictly verified. Although this is a coincidence, most opacity regimes give a scaling not very different from unity. One must nevertheless bear in mind that the vertical transport of energy can be also by convection or fully turbulent so that these scalings loose their validity (apart that providing the value of B_z since it only used the definition of μ).

Several observational diagnostics could a priori reveal the presence of a magnetized disc driving jets : (i) the measure of a large (organized) disc magnetic field ; (ii) optically thin regions (since τ can be smaller than unity) or some lack of disc emission (since $\chi \sim \varepsilon \ll 1$) ; (iii) a different spectral energy distribution (the effective temperature scales as $r_o^{(\xi-3)/4}$) for discs with a large ejection index ξ. But usually, spectral energy distributions are

[15] Apparently only since in the above radial scalings one must take into account that the disc accretion rate itself varies as $\dot{M}_a \propto r^\xi$.

too tricky to interpret and we don't have the resolution yet to measure disc magnetic fields.

Self-collimated jets

The most acurate tool to discriminate between models is to confront theoretical predictions with recent *spatially resolved* observations of the inner wind structure of TTS in forbidden emission lines of [O I], [S II] and [N II]. Indeed, being optically thin, these lines carry information on both dynamic and thermodynamic properties of the whole volume of emission. So, one way to use this information is to construct the following synthetic observations and comparing them to real ones :

- **Emission maps**, which must then be convolved to typical resolutions in order to predict what would be the observed jet morphology and collimation properties (eg. displacement of emission peaks, jet FWHM as a function of distance).
- **Line profiles**, like those obtained using long-slit spectroscopy, and integrated profiles.
- **Integrated line fluxes** as well as their correlations with the disc accretion rate.
- **Forbidden line ratios**, which reflect the values of the electron density, ionisation fraction and local temperature.

While the first two observations offer constraints on the jet dynamics, the last ones test mainly the heating and ionization mechanisms along the jet. We already have a dynamical model providing us with jet density and velocity. The gas emissivity then requires to know the jet thermal and ionization states. With that in hand, we can easily compute synthetic observations and compare them to real ones. This has first been done by Safier (1993) using Blandford & Payne jet solutions. We can now do the same with models of MAES that take self-consistently into account the disc-jet interrelations.

Cabrit et al. (1999), using parametrized temperature and ionization fraction, produced synthetic maps and long-slit spectra that were nicely compatible with observations (Shang et al. (1998) did the same for X-winds). But more reliable predictions require actually solving for the jet thermal and ionization state, given some local heating mechanism. Our models being stationary, we cannot invoke shocks as being the heating process or argue, following Shang et al (2002), that some sort of small scale turbulence provides a means to dissipate locally the jet kinetic energy. In any case however, this would require the introduction of additional free parameters ! The only self-consistent mechanism, intrinsic to MHD flows of low ionization, is ambipolar diffusion (see Sect. 2.2.2).

Using this (unavoidable) effect to heat up jets, Garcia et al. (2001a,b) solved the energy equation along the jet as well as its ionization state, taking into account several heavy elements (C, N, O, S, Ca, Mg, Fe...), photoionization heating and cooling by Hydrogen recombination lines. They used cold (isothermal) MAES solutions obtained by Ferreira (1997) with $\xi \sim 0.01$. Jet widths and variations in line profiles with distance and line tracer are well reproduced. However, predicted maximum velocities are too high, total densities too low and, as a result, the low-velocity [O I] component is too weak. Thus, denser and slower MHD jets are required, namely "warm" jet solutions.

In the solutions used, ejected plasma reaches its asymptotic speed $u_\infty \simeq \Omega_o r_o \sqrt{2\lambda - 3}$, which is typically 10 times the keplerian speed at the field line footpoint. Even though there is some inclination effect that decreases the observed jet velocity, it is still too large : emission from the jet inner region is important. Thus, one needs to decrease the jet terminal speed, which requires to diminish the magnetic lever arm λ (down to $\lambda \sim 10$ or $\xi \sim 0.1$, see Pesenti et al 2004 and Ferreira et al 2006b), ie. to increase the ejection index ξ (which automatically provides a denser jet). However, models with values of ξ larger than 0.01 require an additional heating at the disc surface, whose origin remains to be worked out.

At this stage, one can have confidence in several things : (1) we know exactly, in a model independent way, how "alpha-like" accretion discs can steadily drive jets ; (2) jet properties (velocity, collimation) are strongly dependent on the mass flux allowed by the disc ; (3) such a mass flux is highly sensitive to the critical disc energy equation ; (4) we don't know if real accretion discs ever meet the required physical conditions for MAES.

The MAES paradigm is based on the assumption that a large scale magnetic field is threading the disc *on a large radial extension*. This ensures some kind of cylindrical geometry (actually a conical Alfvén surface), whereas ejection from a small disc region, as in X-winds (Shu et al. 1994), would provide a spherical expansion of the field lines (and a more or less spherical Alfvén surface). Such a basic fact provides very different jet behaviours (see appendix B in Casse & Ferreira 2000a), but the underlying accretion/ejection mechanism remains exactly the same. As we saw, comparing synthetic to real observations is quite a powerful tool to eliminate MAES models and will probably help to discriminate between "disc winds" and "X-winds" (see Ferreira et al 2006b). We know now that, inside the MAES paradigm, YSOs require active chromospheres and coronae[16]. Such a work must therefore be conti-

[16]Kwan (1997) reached the same conclusion from energetic requirements on the low-velocity component of emission lines.

nued, in the hope that a characterization of their properties can indeed be achieved. In parallel, a thorough theoretical (analytical and numerical) work must be performed to understand how instabilities in magnetized discs may lead to turbulence and anomalous transport.

Chapitre 3

Some research directions

The european Marie Curie network "JETSET" has officially begun February 1st 2005 and will run until 2009. This is a network focused on jets from young stars (on the astrophysical side, it deals also with laboratory experiments). Being the work package manager of one of the five research programs, called "Models of MHD Jets from Young Stars", I spend a significant amount of my time dealing with Young Stars. My research program is therefore shared in two main topics : the study of magnetic star-disc interactions and the dynamical and spectral behavior of microquasars.

3.1 Magnetic star-disc interactions

3.1.1 Astrophysical background

Once they become visible in the optical, T Tauri stars exhibit rotational periods of the order of 10 days, which is much smaller than expected (Bouvier et al. 1997, Rebull et al. 2002). This implies a very efficient mechanism of angular momentum removal from the star during its embedded phase. Moreover, a T Tauri star seems to evolve with an almost constant rotational period although it undergoes some contraction and is still actively accreting disc material for roughly a million years. This is a major issue in star formation, unsolved yet.

One solution to this paradox is the star-disc interaction (Camenzind 1990, Königl 1991). Angular resolution is not yet sufficient to directly image this region (of size 0.1 AU or less : requires optical interferometry) but there are mounting spectroscopic and photometric evidences that the disc is truncated by a stellar magnetosphere and that accretion proceeds along magnetic funnels or curtains towards the magnetic poles (Bouvier et al. 2007). This gave

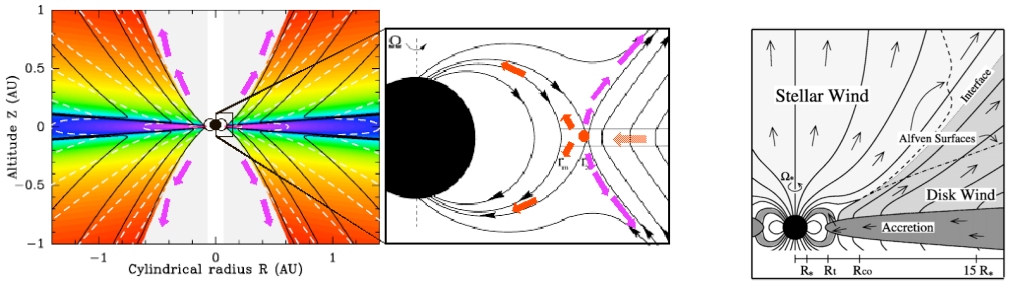

FIG. 3.1 – **Left and center :** Star-disc interaction where the stellar magnetic moment is parallel to the disc magnetic field. There are three distinct types of ejection : a stellar wind on the axis, a disc wind (MAES shown in colors) and a sporadic reconnection X-wind at the interface, braking down the protostar (Ferreira et al. 2000). **Right :** Star-disc interaction in the anti-parallel case. Here, the stellar spin down is done by a wide open stellar wind, assuming no strong confinement by the outer disc wind (Matt & Pudritz 2005b).

rise to the so-called "disc locking paradigm", where it is assumed that the stellar angular momentum can be transferred to the disc. Unfortunately, this idealized picture can probably not be maintained (see thorough discussion in Matt & Pudritz 2005a). An easy way out is to launch disc material along magnetic field lines that are anchored onto the rotating star.

There are two "simple" ways to achieve this as illustrated in figure 3.1.

The first way is to assume that both the disc and the stellar fields have the same origin, so that the stellar magnetic moment is parallel to the disc magnetic field (fig. 3.1, left). Then, both fields cancel each other at some radius in the disc midplane, giving rise to time dependent ejection events above this reconnection zone. Such a reconnection X-wind (ReX-wind) can efficiently brake down a contracting and accreting protostar on the correct time scales (Ferreira et al. 2000). The second way is to consider an anti-parallel magnetic configuration as proposed by Matt & Pudritz (2005b). Magnetic braking is now due to the fact that the stellar wind is assumed to be wide open, regardless of the presence of the outer confining disc wind (see also Lovelace et al 1999).

The magnetic star-disc interaction is far too complex to be tackled by analytical means and requires the extensive use of heavy numerical MHD experiments. Although there have been already several attempts on these lines (eg. Romanova et al. 2002, Kuker et al. 2003, Long et al. 2005 and references therein), none of the results shown can be reliable because of the crude physical content of the description used for the circumstellar accretion

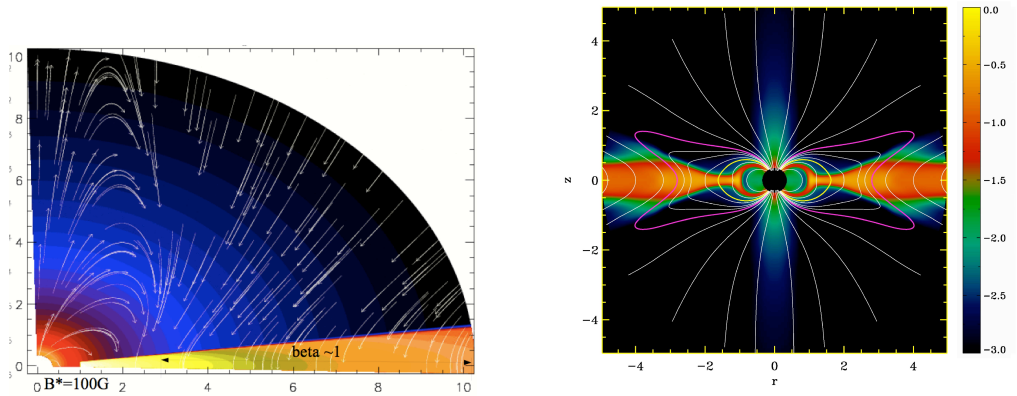

FIG. 3.2 – **Left :** Initial condition of a star-disc simulation done with VAC where the stellar magnetic field is anti-parallel with the disc magnetic field (white lines). Colors show the density distribution. This is the magnetic configuration invoked by Matt & Pudritz (2005b). **Right :** Snapshot of a numerical simulation done with PLUTO of a star-disc interaction with no magnetic field in the disc.The disc truncation as well as the accretion columns are clearly visible. Here, the star is being spun up by the accretion process.

disc. The following questions are therefore still open :

1. **Accretion columns formation :** What are the physical conditions required to allow disc material to flow along stellar field lines ? What determines exactly the disc truncation radius ? What happens if, as observations clearly suggest, the stellar dipole is inclined ?
2. **Magnetic stellar spin down :** What is the dominant mechanism, ReX-wind, stellar wind, something else ? Is disc locking discarded for good ?
3. **Variability :** What is its origin ? Is the star-disc interaction stable ? Can accretion and ejection phases coexist ? If a stellar dynamo is at work, can the two configurations shown in figure 3.1 occur in turn ?

3.1.2 Research projects

The above list of questions defines precisely my research project for young stars. That is quite a huge task but with important implications for star formation.

Addressing reliably these issues cannot be done without a thorough description of the accretion process. My understanding of accretion-ejection pro-

cesses and the physics of magnetized accretion discs gives therefore a strong advantage with respect to other groups. However, one has to master also heavy numerical technics. I have therefore started in this direction and build up a small group around me. It is currently composed of a new PhD student, Nicolas Bessolaz, and a post-doc Claudio Zanni (paid by the JETSET network). I will also promote the recruitment of a young researcher on this promising topic.

Nicolas's PhD thesis started in november 2004 under the joint supervision of J. Bouvier (LAOG), myself and Rony Keppens (Belgium). He is doing 2D simulations using the VAC MHD code. He showed that accretion columns and disc truncation can be done with a stellar magnetic field much smaller than what has been used until now in the literature. A letter reporting this major result is close to submission. He will then study the effect of a large magnetic field in the disc as in figure 3.2. This is the configuration of Matt & Pudritz (2005b) and we will investigate how the presence of a MAES impacts on the mass loading onto the accretion columns.

Claudio Zanni started this post-doc on October 2005. He is using another MHD code, PLUTO, developed at Torino (Italy). We obtained what I think are the only numerical simulations published so far able to provide an unambiguous answer to the magnetic spin down problem (question 2 above). The simulations clearly show how the magnetic torques behave (figure 3.2) : without ejection, the star-disc interaction can only lead to a magnetic spin up of the star. We are currently scanning the parameter space and study the effect of initial conditions in order to have definite results on that crucial topic. A paper is in preparation. In a second step, we will address the 3D star-disc interaction, which is a real numerical challenge. The astrophysical goal is of course to study inclined dipoles but non-axisymmetric accretion onto a 2D dipole would be also relevant.

Observers are strongly interested by these results and projects, in particular the 3D aspects. On a mid-term, one would then need to design numerical tools in order to construct synthetic observations such as emission maps in lines or in the continuum. Another prospect would be to use a stellar magnetic field such as those reconstructed from Doppler-Zeeman measurements. I have strong links with J.-F. Donati (Toulouse) and M. Jardine (St Andrews, Ecosse) so this could be done once a robust 3D MHD code has been successfully tested in the star-disc context.

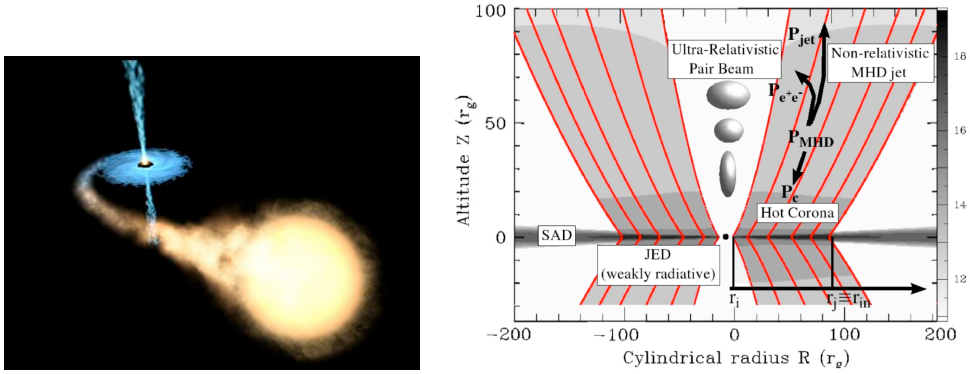

FIG. 3.3 – **Left :** Artist's view of a low mass X-ray binary. The accretion disc settled around the compact object (either a black hole or a neutron star) is fed by the companion's mass and emits a characteristic radiation in the soft X rays ($\sim$ keV). Anti-correlated phases of accretion and ejection are commonly observed. The radio emission attributed to the jets is detected only when the disc emission is lacking. **Right :** Sketch of the unified paradigm proposed by Ferreira et al (2006a). A standard accretion disc (SAD) turns into a jet emitting disc (JED) at some transition radius. The JED puts most of the accretion energy into the jets, resulting in a missing emission in the soft X ray band. Under some circumstances, electron-positron pairs can be created along the jet axis. Note that the grey background is a calculated density stratification, while magnetic field lines are shown in red.

3.2 Dynamical and spectral behavior of microquasars

3.2.1 Astrophysical background

Low mass X-ray binaries are systems made of a normal star and a compact companion, a stellar black hole or a neutron star, in orbit around each other. A fraction of the stellar mass flows towards the compact object and forms an accretion disc (figure 3.3), which disc emits a characteristic thermal emission in the soft X-ray band ($\sim$ keV). Microquasars (Mirabel & Rodriguez 1998) are a subclass of X ray binaries, where bipolar jets are also observed like in GX 339-4, XTE 1550-564, GRS 1915+105, GRO J1655-40, 1E1740.7-2942...

Jets can be either directly imaged (like in figure 1.1) or only detected through an unresolved non-thermal synchrotron emission, ranging from hard X-rays ($\sim$ 100 keV) to radio wavelengths. The puzzling thing with microquasars is that accretion and ejection signatures are anti-correlated (Remillard

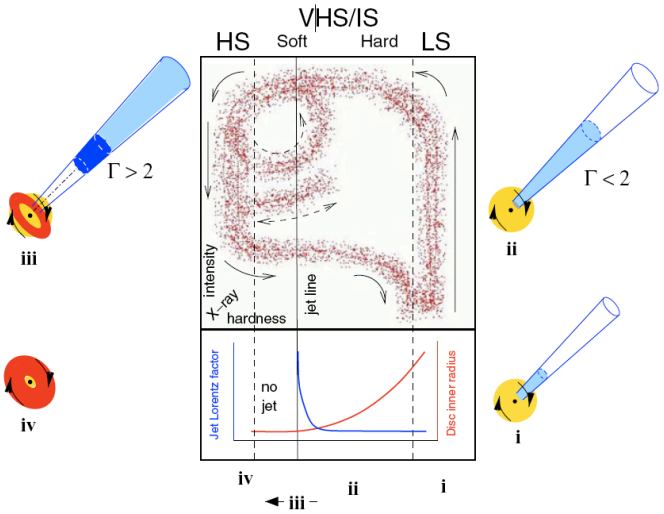

FIG. 3.4 – The hysteresis behavior is clearly seen in this Hardness-Intensity diagram proposed by Fender et al (2004) for X-ray binaries (much alike the H-R diagram for stars). A quiescent object of low luminosity enters an outburst phase and shows a Low (Hard) State with radio jets. It evolves towards an Intermediate State with sporadic and sometimes super-luminal ejections, then a High (Soft) State with no jets but strong disc emission. When the luminosity decreases, it goes back to the quiescent regime but with no sign of ejection. Up to 16 HID of this kind have been obtained for X-ray binaries (Fender, private communication).

& McClintock 2006). Indeed, these objets are observed in spectral states with no signature of ejection but a strong one coming from the disc (High/Soft states) and others where the disc emission is absent but with a strong jet signature (Low/Hard states), sometimes even super-luminal sporadic ejections. Moreover, these various spectral states have quite distinctive timing properties such as quasi-periodic oscillations, which are only observed during the jet states. Moreover, there is clearly an indication that they are following some hysteresis (eg. Remillard & McClintock 2006), as displayed in figure 3.4.

This rich phenomenology is a challenge for theoreticians. Despite many attempts addressing only one aspect of the situation, there was no model or picture describing all the spectral and timing properties of microquasars as emerging from *a global and coherent dynamical system.*

This is what my collaborators and myself proposed recently (Ferreira et al 2006a, figure 3.3). In this paradigm, a large scale magnetic field is advected along with the accretion flow so that a MAES can be established in the

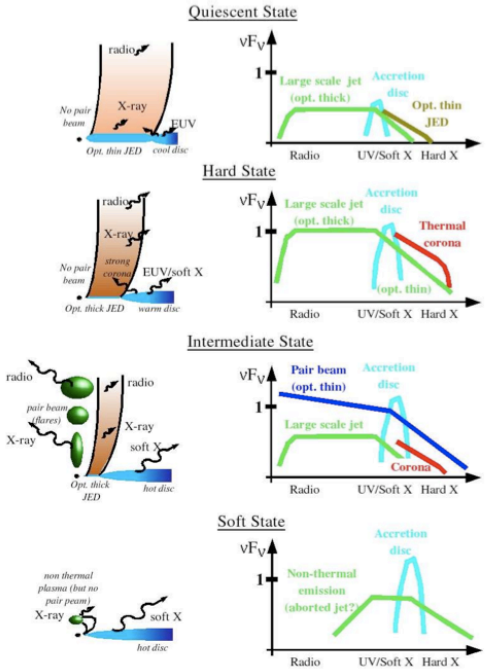

FIG. 3.5 – Sketch of the relative importance of the dynamical constituents (SAD, JED and pairs) of the innermost disc regions and their corresponding spectral energy distribution (right). The time sequence, from top to bottom, would correspond to an increase of the disc accretion rate.

innermost regions. A standard accretion disc (SAD) becomes therefore a jet emitting disc (JED) below some transition radius. Since the JED puts all the accretion power into the jets, the disc emission is drastically reduced, giving rise to an apparent disappearance of the disc signature. We showed that this picture can explain each canonical spectral state and that the transition from one state to another can be readily obtained by varying the disc accretion rate (luminosity) and transition radius (disc magnetic field). This dynamic system has therefore all the physical ingredients required to exhibit an hysteresis.

3.2.2 Research projects

There is much to be done in order to reach a comprehensive understanding of the microquasar phenomenogy. While the paradigm proposed by Ferreira et al (2006a) does seem to be consistent with all known properties, a number of things remain to be proved.

The following projects define more precisely my research activity related

to microquasars.

Spectral energy distributions

Computing SEDs is a necessary step in order to compare our dynamical model with observations. Our goal is to replace the drawings in figure 3.5 by real calculations of both the thermal and non-thermal (Bremsstrahlung, synchrotron and Inverse Compton) emission. This work is done in collaboration with P.-O. Petrucci (LAOG) and Cedric Foellmi, a post-doc who just obtained a 2-years grant on this project from the Swiss government (FNS). The interrelation between accretion and ejection is inherent of the dynamical system (MAES). However, we need to prove, once the disc (soft X rays) and jet (hard X-rays to radio) signatures will be computed, that they fulfill the observed correlations (Corbel et al. 2003).

The microquasars hysteresis

This is a typical behavior of a dynamical system forced to go through bifurcations when one or more control parameters gently evolved with time. A chaotic behavior can even sometimes emerge. I started to study this amazingly interesting feature of microquasars with Guy Pelletier (LAOG). Our leading expertise of MAES allowed us to greatly simplify the set of MHD equations in order to obtain a new set of time-dependent equations. The dynamics imply the advection of the large scale magnetic field within the disc and in particular towards the central object. This raises the issue of the magnetic coupling to a black hole's magnetosphere. Although the effect of inward magnetic field advection can be quite easily modeled when the central object is a neutron star (the work underwent for young stars can be directly applied), everything remains to be done for a black hole.

Effect of the pair beam on the MHD jet

In our model, electron-positron pairs can be created within the core of the MHD jet and accelerated up to relativistic speeds by the Compton rocket. However, a catastrophic pair creation may sometimes be triggered with the sudden release of energy. This may have a drastic effect on the MHD jet and even destroy it. To test this hypothesis, we hired in October 2006 Gareth Murphy as a 3 year post-doc on an ANR grant (project *Astro2flots*, PI : P.-O. Petrucci). In collaboration with G. Henri and P.-O. Petrucci, we will make MHD simulations of an accretion-ejection structure (such as those in figure 1.4) perturbed by a highly variable and energetic inner flow.

Understanding microquasars has important consequences on some other astrophysical fields. This is because these objects offer unique constraints on the physics of accretion-ejection. Indeed, the observed cycles or durations of each spectral state are much longer than the inferred keplerian times. For instance, even the fastest evolving microquasar, namely GRS 1915+105, exhibits duty cycles of 20-30 minutes whereas the dynamical time scale is of the order of several milliseconds. We are thus probing "secular" evolutions of accretion-ejection systems. These evolutions would be absolutely unobservable in AGN where the expected time scales would be up to 100 million times longer. Therefore each quasar or galaxy is frozen in a particular spectral state. Understanding these states in microquasars will certainly provide deep insights in the physics and classification of AGN. That may as well be also the case for Young Stars. T Tauri stars, along their history, go through several phases of strong accretion events with no signature of large jets (as in FU Ori, for instance), very much alike High/Soft states in microquasars...

Bibliographie

Balbus, S. A. & Hawley, J. F. 1991, ApJ, 376, 214

Balbus, S.A. 2003, ARA&A, 41, 555

Banerjee, R. & Pudritz, R.E, 2006, ApJ, 641, 949

Bell K.R., Lin D.N.C. 1994, ApJ 427, 987

Blandford R.D., Rees M.J. 1974, MNRAS 169, 395

Blandford R.D. 1976, MNRAS 176, 465

Blandford, R. D. & Payne, D. G. 1982, MNRAS, 199, 883

Bouvier, J., Forestini, M., & Allain, S. 1997, A&A, 326, 1023

Bouvier, J., Alencar, S. H. P., Harries, T. J., Johns-Krull, C. M., & Romanova, M. M. 2007, in Protostars and Planets V, ed. B. Reipurth, D. Jewitt, & K. Keil, 479–494

Brandenburg A., Donner K.J. 1997, MNRAS 288, L29

Breitmoser E., Camenzind M. 2000, A&A 361, 207

Bridle, H.A., Perley, A.R., 1984, ARA&A, 22, 319

Cabrit, S., Edwards, S., Strom, S. E., & Strom, K. M. 1990, ApJ, 354, 687

Cabrit S., Ferreira J., Raga A.C. 1999, A&A 343, L61

Camenzind M. 1990, in G. Klare (ed.), Rev. in Modern Astrophysics, 3, Springer-Verlag, Berlin

Cantó J. 1980, A&A 86, 327

Cao X., Jiang D.R. 1999, MNRAS 307, 802

Casse, F. & Ferreira, J. 2000a, A&A, 353, 1115

Casse, F. & Ferreira, J. 2000b, A&A, 361, 1178

Casse, F. & Keppens, R. 2002, ApJ, 581, 988

Casse, F. & Keppens, R. 2004, ApJ, 601, 90

Chan K.L., Henriksen R.N. 1980, ApJ 241, 534

Contopoulos, J. & Lovelace, R. V. E. 1994, ApJ, 429, 139

Contopoulos J., Sauty C. 2001, A&A 365, 165

Corbel, S., Nowak, M. A., Fender, R. P., Tzioumis, A. K., & Markoff, S. 2003, A&A, 400, 1007

Crutcher R.M. 1999, ApJ 520, 706

DeCampli, W. M. 1981, ApJ, 244, 124

Donati, J.-F., Paletou, F., Bouvier, J., Ferreira J. 2005, Nature, 438, 466

Fender, R. P., Belloni, T. M., & Gallo, E. 2004, MNRAS, 355, 1105

Fendt C., Camenzind M., Appl S. 1995, A&A 300, 791

Fendt C., Elstner D. 2000, A&A 363, 208

Ferreira, J. & Pelletier, G. 1993a, A&A, 276, 625

Ferreira, J., Pelletier, G., 1993b, A&A, 276, 637

Ferreira, J. & Pelletier, G. 1995, A&A, 295, 807

Ferreira, J. 1997, A&A, 319, 340

Ferreira, J., Pelletier, G., & Appl, S. 2000, MNRAS, 312, 387

Ferreira, J. 2002, in "X Summer School on Stellar Physics", J. Bouvier & J.-P. Zahn (Eds), EDP Science, astro-ph/0311621

Ferreira, J. & Casse, F. 2004, ApJ, 601, L139

Ferreira, J., Petrucci, P.-O., Henri, G., Saugé, L., & Pelletier, G. 2006, A&A, 447, 813

Ferreira, J., Dougados, C., & Cabrit, S. 2006a, A&A, 453, 785

Galeev, A.A., Rosner, R., & Vaiana, G.S., 1979, ApJ, 229, 318

Garcia, P. J. V., Ferreira, J., Cabrit, S., & Binette, L. 2001a, A&A, 377, 589

Garcia, P. J. V., Cabrit, S., Ferreira, J., & Binette, L. 2001b, A&A, 377, 609

Gomez de Castro A.I., Pudritz R.E. 1993, ApJ 409, 748

Goodman A.A., Benson P.J., Fuller G.A., Myers P.C. 1993, ApJ 406, 528

Hartigan, P., Edwards, S., & Ghandour, L. 1995, ApJ, 452, 736

Hartmann, L. & MacGregor, K. B. 1980, ApJ, 242, 260

Heyvaerts J., Priest E.R. 1989, A&A 216, 230

Heyvaerts, J. & Norman, C. 1989, ApJ, 347, 1055

Heyvaerts, J. & Norman, C. 2003, ApJ, 596, 1270

Heyvaerts J., Priest E.R., Bardou A. 1996, ApJ 473, 403

Jones D.L., Werhle A.E., Meier D.L., Piner B.G. 2000, ApJ 534, 165

Königl A. 1982, ApJ 261, 115

Königl A. 1986, Can. J. Phys. 64, 362

Königl A. 1991, ApJ 370, L39

Krasnopolsky, R., Li, Z.-Y., & Blandford, R. 1999, ApJ, 526, 631

Kudoh T., Matsumoto R., Shibata K. 1998, ApJ 508, 186

Küker, M., Henning, T., & Rüdiger, G. 2003, ApJ, 589, 397

Kwan, J. 1997, ApJ, 489, 284

Lery T., Henriksen R.N., Fiege J.D. 1999, A&A 350, 254

Lery T., Heyvaerts J., Appl S., Norman C.A. 1999, A&A 347, 1055

Li J. 1996, ApJ 456, 696

Li Z.-Y. 1995, ApJ, 444, 848

Li Z.-Y. 1996, ApJ 465, 855

Livio, M. 1997, in ASP Conf. Ser. 121 : IAU Colloq. 163 : Accretion Phenomena and Related Outflows, ed. D. T. Wickramasinghe, G. V. Bicknell, & L. Ferrario, 845

Long, M., Romanova, M. M., & Lovelace, R. V. E. 2005, ApJ, 634, 1214

Lovelace R.V.E. 1976, Nature 262, 649

Lovelace R.V.E., Wang J.C.L., Sulkanen M.E. 1987, ApJ 62, 1

Lovelace R.V.E., Romanova M.M., Bisnovatyi-Kogan G.S. 1999, ApJ 514, 368

Machida M., Hayashi M.R., Matsumoto R. 2000, ApJ, 532, L67

Masset, F.S., Morbidelli A., Crida, A., Ferreira J. 2006, ApJ, 642, 478

Matt, S. & Pudritz, R. E. 2005a, ApJ, 632, L135

Matt, S. & Pudritz, R. E. 2005b, MNRAS, 356, 167

McClintock, J. E. & Remillard, R. A. 2003, astro-ph/0306213

Mestel L. 1968, MNRAS 138, 359

Miller K.A., Stone J.M. 2000, ApJ 584, 398

Mirabel, I. F. & Rodriguez, L. F. 1998, Nature, 392, 673

Mirabel I.F.,Rodriguez L.F. 1999, ARA&A 37, 409

Okamoto I. 1999, MNRAS 307, 253

Okamoto, I. 2003, ApJ, 589, 671

Ostriker, E. C. 1997, ApJ, 486, 291

Ouyed, R. & Pudritz, R. E. 1997a, ApJ, 482, 712

Ouyed, R. & Pudritz, R. E. 1997b, ApJ, 484, 794

Ouyed, R. & Pudritz, R. E. 1999, MNRAS, 309, 233

Ouyed, R., Clarke, D.A., and Pudritz, R. E. 1997, ApJ, 482, 712

Parker E.N. 1958, ApJ 128, 664

Pelletier G., Pudritz R.E 1992, ApJ 394, 117

Pesenti N., Dougados C., Cabrit S., O'Brien D., Garcia P., Ferreira J. 2003, A&A, 410, 155

Pesenti, N., Dougados, C., Cabrit, S., et al. 2004, A&A, 416, L9

Pudritz, R.E., Norman C.A. 1983, ApJ 274, 677

Pudritz, R. E., Rogers, C.S. and Ouyed, R. 2006, MNRAS, 365, 1131

Ray, T. P., Mundt, R., Dyson, J. E., Falle, S. A. E. G., & Raga, A. C. 1996, ApJ, 468, L103

Rebull, L. M., Wolff, S. C., Strom, S. E., & Makidon, R. B. 2002, AJ, 124, 546

Remillard, R. A. & McClintock, J. E., 2006, ARA&A, 44, 49,

Rekowski M.v., Rüdiger G., Elstner D. 2000, A&A 353, 813

Romanova, M. M., Ustyugova, G. V., Koldoba, A. V., & Lovelace, R. V. E. 2002, ApJ, 578, 420

Rosso F., Pelletier G. 1994, A&A 287, 325

Safier P.N. 1993, ApJ 408, 115

Sauty, C. & Tsinganos, K. 1994, A&A, 287, 893

Sauty, C., Trussoni, E., & Tsinganos, K. 2002, A&A, 389, 1068

Sergeant S., Rawlings S., Maddox S.J., Baker J.C., Clements D., Lacy M., Lilje P.B. 1998, MNRAS 294, 494

Shakura, N. I. & Sunyaev, R. A. 1973, A&A, 24, 337

Shakura N.I., Sunyaev R.A., Zilitinkevich S.S. 1978, A&A 62, 179

Shang, H., Shu, F. H., & Glassgold, A. E. 1998, ApJ, 493, L91

Shang, H., Glassgold, A. E., Shu, F. H., & Lizano, S. 2002, ApJ, 564, 853

Shibata K., Uchida Y. 1985, PASJ, 37, 31

Shu, F. H., Najita, J., Ruden, S. P., & Lizano, S. 1994b, ApJ, 429, 797

Shu, F. H., Najita, J., Ostriker, E. C., & Shang, H. 1995, ApJ, 455, L155

Spruit H.C., Foglizzo T., Stehle R. 1997, MNRAS 288, 333

Stone, J. M. & Norman, M. L. 1994, ApJ, 433, 746

Tagger M., Pellat R. 1999, A&A 349, 1003

Tagger, M., Varnière, P., Rodriguez, J., & Pellat, R. 2004, ApJ, 607, 410

Uchida Y., Shibata K. 1984, PASJ 36, 105

Ustyugova G.V., Koldoba A.V., Romanova M.M., Chechetkin V.M., Lovelace R.V.E. 1999, ApJ 516, 221

Ustyugova G.V., Lovelace R.V.E., Romanova M.M., Li H., Colgate S.A. 2000, ApJ 541, L21

Vlahakis, N., Tsinganos, K., Sauty, C., & Trussoni, E. 2000, MNRAS, 318, 417

Wardle, M. & Königl, A. 1993, ApJ, 410, 218

Yoshizawa, A., Yokoi, N., 1993, ApJ, 407, 540

Zanni, C., Ferrari, A., Massaglia, S., Bodo, G., & Rossi, P. 2004, Ap&SS, 293, 99